2016-04

Theoretical study of structural and thermodynamic properties of gaseous metal hydrides m2xh4 (m = li, na; x = be, mg)

Shomari, Awadhi

THEORETICAL STUDY OF STRUCTURAL AND THERMODYNAMIC PROPERTIES OF GASEOUS METAL HYDRIDES M$_2$XH$_4$ (M = Li, Na; X = Be, Mg)

Awadhi Shomari

A Dissertation Submitted in Partial Fulfilment of the Requirements for the Degree of Master's in Materials Science and Engineering of the Nelson Mandela African Institution of Science and Technology

Arusha, Tanzania

April, 2016

ABSTRACT

This study aimed to explore the properties of the complex hydrides which seem to be the promising candidates for hydrogen storage materials. The geometrical structure, vibrational spectra and thermodynamic characteristics of the gaseous complex hydrides, MXH_3 and M_2XH_4 (M = Li, Na; X = Be, Mg) and the subunits LiH, NaH, Li_2H^+, Li_2H^+, Li_2H_2, Na_2H_2, BeH_2, MgH_2, MgH_3^-, BeH_3^- have been investigated. Quantum chemical methods of density functional theory and second order Moller−Plesset perturbation theory have been applied. According to the calculations, three isomers of M_2XH_4 have been proved to exist, polyhedral of C_{2v} symmetry; two−cycled, D_{2d} and hexagonal shape, C_{2v}. For M_2BeH_4 polyhedral isomer was found to have the lowest energy and for M_2MgH_4 was cyclic hexagonal configuration. The abundance of the isomers in vapour was evaluated and the hexagonal isomer was observed to prevail in vapour both for beryllium and magnesium complexes. For smaller hydrides, MXH_3, the cyclic equilibrium structure (C_{2v}) was shown to exist, another possible configuration, the linear one ($C_{\infty v}$) was found to be of much higher energy (~130 kJ mol^{-1}).

Different pathways of gas−phase and heterophase dissociation reactions were examined; the enthalpies of formation of the complex hydrides were found; 105 ± 26 (LiBeH$_3$), 63 ± 37 (Li$_2$BeH$_4$), 121 ± 27 (NaBeH$_3$), 117 ± 39 (Na$_2$BeH$_4$), 114 ± 13 (LiMgH$_3$), 113 ±12 (Li$_2$MgH$_4$), 162 ± 11 (NaMgH$_3$), and 175 ± 26 (Na$_2$MgH$_4$) (in kJ mol^{-1}). The assessment of thermal stability of the hydrides was done through Gibbs free energies for heterophase decomposition.

DECLARATION

I, **AWADHI SHOMARI** do hereby declare to the Senate of The Nelson Mandela African Institution of Science and Technology that this dissertation is my own original work and that it has neither been submitted nor being concurrently submitted for degree award in any other institution.

_____   _____

Name and signature of candidate   **Date**

The above declaration is confirmed

_____   _____

Name and signature of supervisor   **Date**

_____   _____

Name and signature of supervisor   **Date**

COPYRIGHT

CERTIFICATION

The undersigned certifies that they have read and hereby recommend for final submission in an acceptable form a dissertation entitled *"***Theoretical study of structural and thermodynamic properties of gaseous complex metal hydrides M_2XH_4 (M= Li, Na; X= Be, Mg)***"* in partial fulfillment of the requirements for the Degree of Master's in Materials Science and Engineering of the Nelson Mandela African Institution of Science and Technology.

_____   _____

Prof. Alexander Pogrebnoi   **Date**

(Supervisor 1)

_____   _____

Prof. Tatiana Pogrebnaya   **Date**

(Supervisor 2)

ACKNOWLEDGEMENT

DEDICATION

I dedicate this work to my father, the late Mzee Mpopochoo, my mother, Dotto Kimwaga, my beloved wife, Patima Vuai Haji and my four cute daughters who are my treasure (Salma, Mariam, Rahma and Asia).

TABLE OF CONTENTS

Contents   **Page**

LIST OF TABLES

LIST OF FIGURES

LIST OF APPENDICES

LIST OF ABBREVIATIONS AND SYMBOLS

Abbreviation and Symbols

IR	Infrared
DFT	Density Functional Theory
MP2	Møller–Plesset Perturbation theory of 2nd order
B3PW91	Becke–Perdew/Wang 91 Functional
B3P86	Becke–Perdew Functional
GAMESS	General Atomic and Molecular Electronic Structure System
NIST	National Institute of Standards and Technology
ω_i	Vibration frequency
μ_e	Dipole moment
R_e	Internuclear distance
Å	Angstrom (10^{-10} m)
H	Planck's constant
$\Delta_r H°(0)$	Enthalpy of dissociation
$\Delta_f H°(0)$	Enthalpy of formation
$\Delta_s H°(0)$	Enthalpy of sublimation
$\Delta_r G°(T)$	Gibbs free energy
c	Speed of light
T	Absolute Temperature (K)
$\Phi°(T)$	Reduced Gibbs free energies
$S°(T)$	Entropy
$H°(T)-H°(0)$	Enthalpy increment
I	Infrared intensities
$\Delta\varepsilon$	Zero point vibration energy (ZPVE) correction
$\Delta_r E$	Energy of reaction
Γ	Total vibrational frequencies representation
E	Total electron energy
$\alpha_e, \beta_e, \delta_e, \gamma_e$	Valence angle representation

CHAPTER ONE

Introduction

This chapter describes the general introduction of the study. It mainly focuses on the background information, research problem, objectives, research questions and significance of the study.

1.1 Background Information

Hydrogen is one of the leading candidates as an energy carrier of the future because of its high energy content and clean burning, potentially renewable nature. A particularly daunting challenge facing its use in transportation, however, is the development of a safe and practical storage system (Dincă and Long, 2008). Recent research on hydrogen storage has been guided by the requirements set forth by the United States Department of Energy in 2003 and amended in 2006 (Milliken, 2007). The methods of interest include compression, liquefaction, physisorption, metallic hydrides, and complex hydrides, which are commented with respect to the technical state and the viability in future application (Zhou, 2005). Hydrogen storage remains one of the more challenging technological barriers to the advancement of hydrogen fuel cell technologies for mobile applications (Graetz, 2012).

Züttel proposed two criterions for hydrogen storage materials; the first one is to pack hydrogen as close as possible, which means to minimize the volume of hydrogen and the second one is the reversibility of hydrogen uptake and release with the exclusion of all covalent hydrogen−carbon compounds (Züttel, 2003). Several reversible hydrogen storage methods have been illustrated such as; high pressure gas cylinders, liquid hydrogen in cryogenic tanks, adsorbed hydrogen, absorbed of hydrogen on interstitial sites in a host metal, complex compounds, metals and complexes together with water (Züttel, 2003). Practical hydrogen storage materials must exhibit favorable thermodynamic properties and have sufficiently rapid kinetics of hydrogen charging and discharging (Alapati *et al*., 2006). Moreover, it has been reported that the equilibrium between gaseous H_2 and a metal hydride is determined by both enthalpic and entropic contributions to the system's free energy, enthalpy alone provides a useful means to screen candidate materials (Grochala and Edwards, 2004).

It was reported that with technological progress in algorithms and computer hardware, first−principles calculations based on the density functional theory (DFT) with the use of the local density approximation (LDA) or generalized gradient approximation (GGA) can not only explain the already known properties of a given material but also resolve the ambiguities in experimental structural determination (Hu *et al*., 2007). This has made material design become realistic.

The methods that have been investigated for hydrogen storage are separated into two groups: the storage of molecular or atomic/ionic hydrogen (Chater, 2010). A hydrogen storage system for molecular hydrogen increases the volumetric density by physical compression of the gas, by liquefaction or by adsorption on surfaces. Atomic hydrogen can be stored by reaction of hydrogen gas to form metal hydrides or complex hydrides (Chater, 2010). Most hydrogen storage materials can be divided into two categories, those that bind molecular hydrogen to surfaces via weak dipole (van der Waals) interactions in a process known as physisorption (e.g., activated carbons and metal organic frameworks and those that trap atomic hydrogen via a strong chemical bond (e.g., metal hydrides, complex hydrides and chemical hydrides) (Graetz, 2012).

Complex metal hydrides such as alanates and borohydrides contain a large amount of hydrogen and are considered as promising materials for hydrogen storage (Jena, 2015). Superalkalines molecules being characterized by lower ionization potential have seen as good candidate in synthesis of non−tradition salt (metal hydride) (Pathak *et al*., 2011). The discovery of the superatoms by (Giri *et al*., 2014) paved the way to the synthesis of new class of materials called supersalts or complex hydrides which seemed to be good candidate for hydrogen storage materials.

Computer simulations allow for the investigation of many materials properties and processes that are not easily accessible in the laboratory. First−principles techniques based on density−functional theory (DFT) are much more predictive, not being biased by any prior experimental input, and have demonstrated a considerable accuracy in a wide class of materials and variety of external conditions. The proposed work therefore sought to investigate the quantum chemical study of metal hydrides, MXH_3 and M_2XH_4 (M = Li, Na; X = Be, Mg) for hydrogen storage materials.

1.2 Research problem

Fossil fuels as the main source of energy worldwide are depleting, unsteady in terms of price, and have a negative impact to both the environment and humans beings (Union, 2008). As such, there has been a strong push to switch to, and a growing research interest, both in academia and industry, in renewable energy sources such as wind, hydro, solar and storage materials. Unlike fossil fuels, renewable energy sources are sustainable due to their infinite abundance and little or zero carbon emission. Hydrogen shows a promising interest as a synthetic fuel because it is lightweight, highly abundant and its oxidation product (water) is environmentally benign, but storage remains a problem. Various efforts have been done to investigate structural, electronic and thermodynamic properties of crystalline structure of metal hydrides as hydrogen storage materials. However, a few studies have been done to investigate these properties of metal hydride in gaseous or vapour form. This research aims at investigating these parameters so as to widen the theoretical understanding of the metal hydride as hydrogen storage materials.

1.3 Objective

1.3.1 General objective

The main objective of the research was to investigate the properties of some gaseous metal hydrides by quantum chemical methods.

1.3.2 Specific objectives

i)   To determine equilibrium geometrical structure and vibrational spectra of some metal hydrides M_2XH_4 (M=Li, Na: X=Be, Mg).

ii)   To examine constituents of metal hydrides.

iii) To determine thermodynamic properties of the selected metal hydrides.

iv)   To examine the dissociation reactions of the selected metal hydrides.

v)   To investigate the thermodynamic stability of the molecules with respect to different channels of decomposition.

vi)   To propose the better material regarding the optimal conditions of H_2 formation on the basis of theoretical results.

1.4 Research questions

(i)   What is the equilibrium geometrical structure and vibrational spectra of some metal hydrides M_2XH_4 (M=Li, Na: X=Be, Mg)?

(ii)   What are the properties of the metal hydrides subunits?

(iii) What are thermodynamic properties of the metal hydrides?

(iv)   What are the dissociation energies of the selected metal hydrides?

(v)   How thermodynamically stable are the metal hydrides for hydrogen storage materials?

(vi)   What are the best materials regarding the optimal conditions of H_2 formation on the basis of theoretical results?

1.5 Significance of the research

The proposed study has helped to provide a detailed understanding or useful information on the structural and thermodynamic properties of the species. It has also helped to provide knowledge and strategies needed to study properties of complex hydrides in gaseous state. These strategies can create skills and expertise in hydrogen storage materials. In addition the skills and knowledge acquired is expected to be transferred to other energy field and provide library of information for publication and opening the new venue for further researches.

CHAPTER TWO

Gaseous Metal Hydrides MBeH$_3$ and M$_2$BeH$_4$ (M = Li, Na): Quantum Chemical Study of Structure, Vibrational Spectra and Thermodynamic Properties[1]

Abstract: The theoretical study of complex hydrides MBeH$_3$ and M$_2$BeH$_4$ (M = Li, Na) have been carried out using DFT MP2 methods with basis set 6−311++G(d, p). The optimized geometrical parameters, vibrational spectra and thermodynamic properties of the hydrides and subunits MH, M$_2$H$^+$, M$_2$H$_2$, BeH$_2$, BeH$_3^-$ have been determined. Two geometrical configurations, cyclic (C_{2v}) and linear ($C_{\infty v}$), were found for pentaatomic MBeH$_3$ molecules, the cyclic isomer being predominant. Three isomers of M$_2$BeH$_4$ molecules were revealed of the following shapes: two−cycled (D_{2d}), polyhedral (C_{2v}) and hexagonal (C_{2v}). Among these structures polyhedral isomer was found to have the lowest energy. The relative abundance of the M$_2$BeH$_4$ isomers in saturated vapour was analyzed. The enthalpies of formation $\Delta_f H°(0)$ of complex hydrides in gaseous phase were determined (in kJ·mol^{-1}): 105 ± 26 (LiBeH$_3$), 63 ± 37 (Li$_2$BeH$_4$), 121 ± 27 (NaBeH$_3$), and 117 ± 39 (Na$_2$BeH$_4$). The thermodynamic stability of the hydrides was examined through Gibbs free energies for heterophase decomposition.

2.1 Introduction

Fossil fuels as the main source of energy worldwide are depleting, unsteady in terms of price, and have a negative impact to both the environment and humans beings (Patlitzianas *et al.*, 2008). Hydrogen shows a promising interest as a synthetic fuel. In order to use hydrogen as the source of energy and replacement of fossil fuels; it has to overcome three technical challenges associated with the production, storage and use (Sartbaeva *et al.*, 2011). Chater reported that the problem of hydrogen storage remains as the most challenging (Chater, 2006).

The large−scale deployment of vehicular fuel cells is hindered by the absence of a commercially feasible hydrogen storage technology. A selection of comparatively lightweight, low−cost, and high−capacity hydrogen storage devices must be available in a variety of sizes to meet different energy needs (Alapati *et al.*, 2006). The use of hydrogen as fuel in transport offers the greatest challenge towards system design. The criteria for a practical hydrogen store for mobile applications have been outlined by the U. S. Department of Energy (Ahluwalia *et al.*, 2012).

Complex metal hydrides studied recently considered as promising materials for hydrogen storage

(Jena, 2015). When Bogdanović and Schwickardi (1997) announced the reversibility of the catalyzed sodium alanate $NaAlH_4$ in hydrogen desorption and absorption reactions at ambient condition, several researches (Zaluska *et al*., 1999; Zidan *et al*., 1999; Fletcher *et al* 1999; Sandrock, 2002; Morioka *et al*., 2003) have been focused on alkali complex hydrides particularly in the kinetics viewpoint. The complex hydrides Li_2MH_5 (M = B or Al) were previously studied theoretically and it was shown that these materials are stable at low temperatures and suggested to be potential for hydrogen storage purposes (Tsere *et al*., 2015).

The prediction and synthesis of hydride compound with sufficient amount of hydrogen contents were done in (Nakamori *et al*., 2006). A lithium–hydride bonding in complexes HMgHLiX with different ligands X including hydrogen was studied theoretically at MP2/6−311++G(d, p) level (Li *et al*., 2009). Vajeeston *et al*., (2008) investigated the atomic arrangements, electronic structures and bonding nature within the $MMgH_3$ (M = Li, Na, K, Rb, Cs) series so as to determine the stability of these materials for hydrogen storage applications.

The decomposition of the complex metal hydrides such as the alkali metal tetrahydroborides to release hydrogen gas was reported (Züttel *et al*., 2003) to proceed in the following two channels:

$$MBH_4 \rightarrow MH + BH_3 \tag{1}$$

$$MBH_4 \rightarrow MH + B + 3/2H_2 \tag{2}$$

Theoretical investigation of structural, electronic and thermodynamic properties of crystalline Na_2BeH_4 and the structural transition from $\alpha-$ to $\beta-Na_2BeH_4$ has been performed in (Hu *et al*., 2008).

This study aimed at theoretical investigation of complex hydrides $MBeH_3$ and M_2BeH_4 (M = Li, Na) in gaseous state implying a potential application for hydrogen storage. The content of hydrogen is 15.8% ($LiBeH_3$), 8.6% ($NaBeH_3$), 14.8% (Li_2BeH_4), and 6.8% (Na_2BeH_4). The target was to determine the structure, geometrical parameters, vibrational spectra and thermodynamic properties of the complex hydrides and subunits they composed of and examine the thermodynamic stability of the hydrides with respect to different channels of decomposition. Therefore, our work provided useful information on the structural and thermodynamic properties of the species and contributes to an exploration of the hydrides for hydrogen storage application.

2.2 Computational Details

The calculations were carried by implementing density functional theory (DFT) with hybrid functional B3PW91 (Becke, 1993), and second−order Møller–Plesset perturbation theory (MP2) with the basis set 6−311++$G(d, p)$. In order to find out the accuracy of calculated results, the properties of the diatomic alkali metal hydride molecules were computed by using two different DFT hybrid functionals, B3P86 and B3PW91, and MP2 method together with the said basis set; the calculated properties were then compared with available experimental data. The optimization of geometrical parameters and vibrational spectra computations were performed using the PC GAMESS (General Atomic and Molecular Electronic Structure System) program (Schmidt *et al.*, 1993) and Firefly version 8.1.0 (Granovsky). Geometrical structures and IR spectra were visualized using the wxMcMolPlt (Bode *et al.*, 2008) and Chemcraft software (Zhurko and Zhurko, 2013). The thermodynamic functions were determined in rigid rotator−harmonic oscillator approximation by using Openthermo software (Tokarev, 2007−2009).

The enthalpies of dissociation reactions $\Delta_r H°(0)$ were computed using the formulae:

$$\Delta_r H°(0) = \Delta_r E + \Delta_r \varepsilon \tag{3}$$

$$\Delta_r \varepsilon = 1/2 hc (\textstyle\sum \omega_{i\ prod} - \sum \omega_{i\ react}) \tag{4}$$

where $\Delta_r E$ is the energy of the reaction calculated through the total energies E of the species, $\Delta_r \varepsilon$ is the zero point vibration energy (ZPVE) correction, $\sum \omega_{i\ prod}$ and $\sum \omega_{i\ react}$ are the sums of the vibration frequencies of the products and reactants respectively. The enthalpy of formation was computed by the equation:

$$\Delta_r H°(0) = \textstyle\sum \Delta_f H°(0)_{prod} - \sum \Delta_f H°(0)_{react} \tag{5}$$

where $\sum \Delta_f H°(0)_{prod}$ and $\sum \Delta_f H°(0)_{react}$ are enthalpies of formation of products and reactants, respectively. The values of $\sum \Delta_f H°(0)_{react}$ were taken from Ivtanthermo Database (Gurvich *et al.*, 1992). The thermodynamic stability of the complex hydrides was examined through Gibbs free energy $\Delta_r G°(T)$ of dissociation reactions. The values of $\Delta_r G°(T)$ were calculated by the formula:

$$\Delta_r G°(T) = \Delta_r H°(T) - T \Delta_r S°(T) \tag{6}$$

where $\Delta_r H°(T)$ and $\Delta_r S°(T)$ are the enthalpy and entropy of the reaction at temperature T.

2.3 Results and Discussion

2.3.1 *Subunits of Complex Hydrides*

Diatomic molecules, NaH, LiH and H_2. Two DFT hybrid functionals, B3P86 and B3PW91, together with MP2 were used to calculate molecular parameters: equilibrium internuclear distance, normal vibrational frequency, and dipole moment (Table 1). To test the accuracy of the calculated results a comparison with the available experimental data has been done. The calculated parameters do not contradict to the experimental values (Irikura, 2007; NIST; Huber and Herzberg, 1979). Among two DFT methods, B3PW91 and B3P86, the former provided a bit more accurate results. Thereby the results for other species considered are represented as found by DFT/B3PW91 and MP2 methods.

Triatomic molecule BeH_2 and ions M_2H^+ (M = Li, Na).

The characteristics of the BeH_2 molecule are summarized in Table 2. The values obtained by the two methods are generally in agreement with each other and reference data (Gurvich *et al*., 1992). The values of equilibrium internuclear distance by DFT and MP2 are slightly shorter, by 0.007 Å and 0.014 Å, than the experimental value, while the valence asymmetric frequency ω_2 is overrated by 3.2% (DFT) and 5.5% (MP2) respectively compared to experimental magnitude. The structure of the triatomic ions M_2H^+ is linear of $D_{\infty h}$ symmetry (Fig. 1 *a*); the results are displayed in Table 3. The experimental reference data are not available.

Table 1. Properties of diatomic molecules

Property	DFT/B3PW91	DFT/B3P86	MP2	Expt
		LiH		
R_e(Li−H)	1.600	1.602	1.594	1.595 (NIST)
−E	8.07468	8.07418	8.02215	
ω_e	1397	1400	1437	1405 (Irikura. 2006)
μ_e	5.8	5.8	6.0	5.9 (NIST)
		NaH		
R_e(Na−H)	1.897	1.895	1.897	1.887 (NIST)
−E	162.81202	162.82073	162.53340	
ω_e	1175	1183	1192	1172 (Irikura. 2006)
μ_e	5.6	5.6	7.1	
		H_2		
R_e(H−H)	0.745	0.748	0.738	0.741 (Huber and Herzberg)
−E	1.17858	1.17973	1.16030	
ω_e	4415	4392	4534	4401 (Huber and Herzberg)

Notes: here and hereafter, R_e is the equilibrium internuclear distance in Å, E is the total energy in au, ω_e is the vibrational frequency in cm^{-1}, μ_e is the dipole moment in D

Table 2. Properties of triatomic molecule BeH$_2$ ($D_{\infty h}$)

Property	DFT/B3PW91	MP2	Expt
R_e (Be−H)	1.333	1.326	1.326 (Jacox, 1994)
−E	15.90487	15.83934	
ω_1 ($\sum_g^+$)	2012 (0)	2064 (0)	
ω_2 ($\sum_u^+$)	2228 (5.8)	2279 (5.94)	2159 (Jacox, 1994)
ω_3 (Π_u)	717 (15.9)	696 (16.8)	698 (Jacox, 1994)

Note: Here and hereafter the parenthesized values near frequencies are intensities of IR spectrum bands, in D^2 amu^{-1} Å^{-2}

The properties calculated follow the trend of that for the diatomic molecules MH (Table 1). It is worth mentioning that the internuclear distance R_e (Li−H) in Li$_2$H$^+$ is longer by ~ 0.05 Å compared to that in LiH and R_e (Na−H) in Na$_2$H$^+$ is longer by ~0.08 Å than that in NaH. The vibration frequencies calculated by two methods are in a good agreement between each other.

Table 3. Properties of triatomic ion, M$_2$H$^+$ (M= Li, Na), D_{∞}h symmetry

Property	DFT/B3PW91	MP2
	Li$_2$H$^+$	
R_e(M−H)	1.649	1.649
−E	15.44642	15.31464
ω_1 ($\sum_u^+$)	428 (0)	443 (0)
ω_2 ($\sum_g^+$)	1670 (11.7)	1720 (12.3)
ω_3 (Π_u)	391 (22.2)	404 (23.9)
	Na$_2$H$^+$	
R_e(M−H)	1.972	1.974
−E	324.93814	324.12418
ω_1 ($\sum_u^+$)	201 (0)	211 (0)
ω_2 ($\sum_g^+$)	1345 (12.6)	1409 (13.3)
ω_3 (Π_u)	357 (21.3)	378 (24.3)

Tetraatomic ion BeH$_3^-$ and molecules M$_2$H$_2$ (M= Li, Na).

The properties of the tetraatomic species are displayed in Tables 4 and 5; their structures are shown in Figs. 1 *b, c*. The tetraatomic ion BeH$_3^-$ has the planar equilibrium configuration of the D_{3h} symmetry. The values obtained through two methods are generally in agreement with each other. For M$_2$H$_2$ molecules, the values of internuclear distances, valence angles, and vibrational frequencies calculated by DFT and MP2 fairly match with each other and with the theoretical results obtained previously (Chen *et al*., 2005). The calculated enthalpy of dimerization for Li$_2$H$_2$ is in agreement within uncertainty limit with the experimental magnitude by (Wu *et al.,* 1982).

Table 4. Properties of tetraatomic BeH$_3^-$ ion, D_{3h} symmetry

Property	DFT/B3PW91	MP2
R_e(Be−H)	1.423	1.415
−E	16.53280	16.44528
ω_1 (A_1')	1673 (0)	1726 (0)
ω_2 (A_2'')	831 (12.8)	870 (13.9)
ω_3 (E')	1673 (42.5)	1726 (43.4)
ω_4 (E')	851 (8.6)	883 (10.1)

Table 5. Properties of dimers M_2H_2 (M=Na, Li), D_{2h} symmetry

Property	Li$_2$H$_2$			Na$_2$H$_2$		
	DFT/B3PW91	MP2	Ref.	DFT/B3PW91	MP2	Ref.
R_e(M−H)	1.756	1.749	1.758	2.115	2.112	2.119
α_e(H−M−H)	99.5	99.6	100	96.8	96.5	96
$-E$	16.22595	16.12348		325.68079	325.12896	
ω_1 (A_g)	1159 (0)	1199 (0)	1194[a]	955 (0)	1004 (0)	993[a]
ω_2 (A_g)	515 (0)	526 (0)	524[a]	225 (0)	230 (0)	228[a]
ω_3 (B_{1g})	886 (0)	911 (0)	902[a]	636 (0)	697 (0)	690[a]
ω_4 (B_{1u})	592 (17.6)	607 (18.6)	604[a]	444 (19.3)	459 (21.5)	458[a]
ω_5 (B_{2u})	967 (22.2)	990 (23.9)	985[a]	783 (22.8)	832 (25.4)	823[a]
ω_6 (B_{3u})	1066 (21.7)	1100 (22.3)	109 [a]	819 (24.1)	869 (25.0)	855[a]
$-\Delta E_{dim}$	201.1	207.9	204[a]	149.0	163.2	
$-\Delta_r H°(0)_{dim}$	186.8	193.2	220 ± 42[b]	140.0	153.0	

Note: Here and hereafter α_e is bond angle in degrees; the values ΔE_{dim} and $\Delta_r H°(0)_{dim}$ are the energies and enthalpies of dimerization reactions 2MH = M$_2$H$_2$ in kJ mol^{-1}; a stands for Chen *et al*., 2005 and b for Wu *et al*., 1982

| (a) | (b) | (c) |
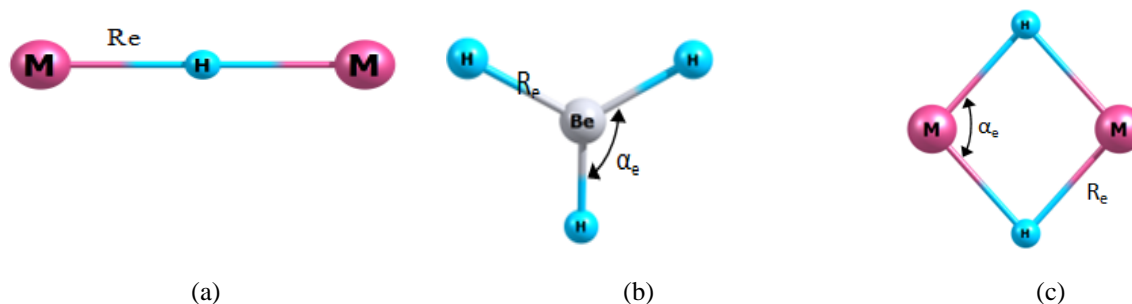
Figure 1. Equilibrium geometrical structure of the species: (a) M$_2$H$^+$ $D_{\infty h}$; (b) BeH$_3^-$, D_{3h}; (c) dimers M$_2$H$_2$, D_{2h}

2.3.2 Geometrical Structure and Vibrational Spectra of Pentaatomic Molecules MBeH$_3$

Two possible geometrical configurations, cyclic (C_{2v}) and linear ($C_{\infty v}$), were considered for pentaatomic MBeH$_3$ molecules (Fig. 2). The calculated equilibrium geometrical parameters and vibrational frequencies for cyclic isomer are shown in Table 6. The binding in the cyclic isomer may be considered through an attachment of M$^+$ cation to BeH$_3^-$ anion. Within the MBeH$_3$ molecules, the fragment BeH$_3$ is distorted compared to free BeH$_3^-$ anion. In the latter the bond lengths and angles are equivalent, R_e(Be−H) ≈ 1,42 Å (Table 4) while in the MBeH$_3$ molecules the bridge distances R_e(Be−H) are elongated to 1.44−1.45 Å; and the terminal distance is shortened to ~1.35 Å; the bond angles become also non−equivalent, the angle β_e(H$_4$−Be$_1$−H$_5$) decreases to 104° in LiBeH$_3$ and 110° in NaBeH$_3$. Thus the BeH$_3$ moieties look alike in both LiBeH$_3$ and NaBeH$_3$ molecules.

The IR spectra of MBeH$_3$ (C_{2v}) molecules are presented in Fig. 3. The similarity of the

vibrational bands is observed for $LiBeH_3$ and $NaBeH_3$. For instance the most intensive bands correspond to the Be−H stretching vibrations at 1528 cm^{-1} ($LiBeH_3$) and 1555 cm^{-1} ($NaBeH_3$). The highest vibration frequencies correspond to the Be_1−H_3 stretching vibrations at 2029 cm^{-1} ($LiBeH_3$) and 1980 cm^{-1} ($NaBeH_3$). The bending vibration H−Be−H is observed at 849 cm^{-1} ($LiBeH_3$) and 833 cm^{-1} ($NaBeH_3$).

(a)   (b)
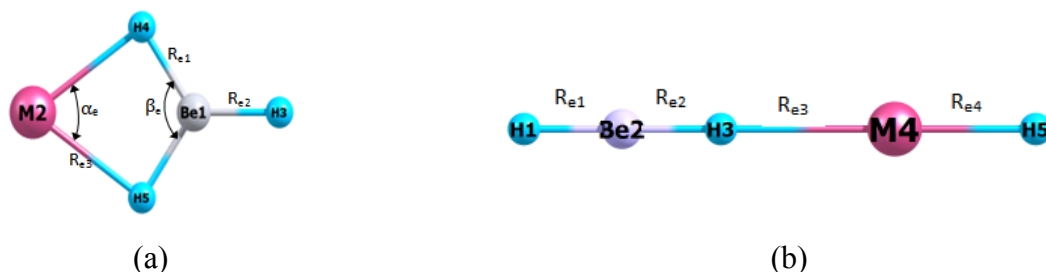
Figure 2. Equilibrium geometrical structure of MBeH$_3$ (M = Li, Na) molecules: (a) cyclic, C_{2v}; (b) linear, $C_{\infty v}$

Table 6. Properties of MBeH$_3$ (M= Li, Na) molecules (C_{2v})

Property	LiBeH$_3$		NaBeH$_3$	
	DFT/B3PW91	MP2	DFT/B3PW91	MP2
R_{e1}(Be$_1$−H$_4$)	1.452	1.446	1.444	1.437
R_{e2}(Be$_1$−H$_3$)	1.352	1.345	1.361	1.355
R_{e3}(M$_2$−H$_5$)	1.740	1.733	2.099	2.097
α_e (H$_4$−M$_2$−H$_5$)	82.5	82.2	69.0	68.3
β_e (H$_4$−Be$_1$−H$_5$)	104.3	103.9	110.7	109.9
$-E$	24.05487	23.93721	178.78495	178.44385
ω_1 (A_1)	2029 (7.08)	2078 (7.52)	1980 (7.41)	2026 (8.38)
ω_2 (A_1)	1622 (6.10)	1667 (6.59)	1618 (7.16)	1665 (7.99)
ω_3 (A_1)	1207 (9.94)	1252 (10.9)	1114 (4.88)	1160 (6.39)
ω_4 (A_1)	594 (1.32)	606 (1.41)	389 (1.18)	394 (1.24)
ω_5 (B_1)	1528 (13.8)	156 1(14.6)	1555 (15.3)	1595 (16.5)
ω_6 (B_1)	1106 (3.09)	1142 (3.65)	982 (3.64)	1017 (4.23)
ω_7 (B_1)	579 (0.72)	604 (0.76)	492 (0.38)	513 (0.39)
ω_8 (B_2)	849 (10.2)	882 (11.0)	833 (10.6)	868 (11.6)
ω_9 (B_2)	327 (0.09)	337 (0.05)	266 (0.04)	265 (0.02)

The properties of the MBeH$_3$ molecules of linear configuration are shown in Table 7. The linear isomer MBeH$_3$ should be represented by linking MH and BeH$_2$ molecules. For lithium bonding complexes HMgH···LiH the linear structure was considered in (Li *et al*., 2009), while existence of possible isomers had not been taken into account. Our results for MBeH$_3$ show that the energy of the linear isomer appeared to be much higher compared to the cyclic one, by 165 kJ mol^{-1} (MP2, both for LiBeH$_3$ and NaBeH$_3$). It is also worth to note a low frequency of vibration ω_7 which corresponds to bending of the Li−H−Be fragment. Moreover, when the parameters of the linear isomers were calculated using DFT/P3P86 method the imaginary frequency for LiBeH$_3$ was revealed which indicates low stability of the linear structure with

respect to bending deformation. Hence only this cyclic isomer was considered further in examination of thermodynamic properties of $MBeH_3$ hydrides.

(a)   (b)
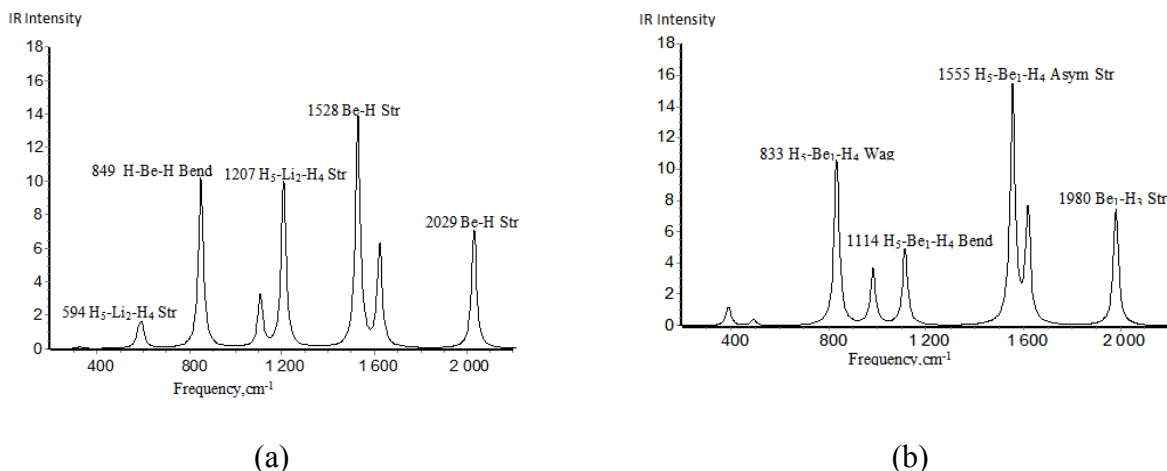
Figure 3. IR spectra of $MBeH_3$ (M = Li, Na) molecules, C_{2v} isomer, calculated by DFT/B3PW91: (a) $LiBeH_3$; (b) $NaBeH_3$

Table 7. Properties of $MBeH_3$ (M= Li, Na) molecules ($C_{\infty v}$)

Property	$LiBeH_3$		$NaBeH_3$	
	DFT/B3PW91	MP2	DFT/B3PW91	MP2
$R_{e1}(Be_2-H_1)$	1.323	1.316	1326	1.318
$R_{e2}(Be_2-H_3)$	1.337	1.328	1.339	1.330
$R_{e3}(M_4-H_3)$	1.914	1.869	2.351	2.299
$R_{e4}(M_4-H_5)$	1.613	1.608	1.909	1.914
$-E$	23.99016	23.87426	178.72323	178.38096
$\Delta_r E_{iso}$	169.9	165.3	162.0	165.1
$\omega_1 (\Sigma^+)$	2283 (9.64)	2343 (10.08)	2255 (8.43)	2317 (9.07)
$\omega_2 (\Sigma^+)$	2082 (1.68)	2145 (1.36)	2038 (1.62)	2106 (1.63)
$\omega_3 (\Sigma^+)$	1366 (7.36)	1396 (7.88)	1151 (8.07)	1169 (9.20)
$\omega_4 (\Sigma^+)$	252 (0.01)	276 (0.03)	142 (0.04)	166 (0.03)
$\omega_5 (\Pi)$	698 (17.3)	701 (17.9)	748 (16.4)	763 (17.4)
$\omega_6 (\Pi)$	214 (6.74)	210 (2.38)	198 (0.93)	226 (0.06)
$\omega_7 (\Pi)$	30 (17.4)	57 (22.3)	77 (20.4)	67 (23.8)

Note: $\Delta_r E_{iso}$ is the relative energy of linear isomer regarding cyclic, $\Delta_r E_{iso} = E_{lin} - E_{cycl}$, in kJ mol^{-1}

2.3.3 Geometrical Structure and Vibrational Spectra of Heptaatomic M_2BeH_4 Molecules

Several different geometrical shapes of the M_2BeH_4 molecules have been considered: bipyramidal one with a tail of C_{2v} symmetry; polyhedral (compact or "hat"−shaped), C_{2v}; two−cycles, D_{2d}; and hexagonal shape, C_{2v}. Among these four configurations, the first one was found to be unstable as imaginary vibrational frequencies were revealed. The rest three structures were proved to correspond to the minima at the potential energy surface and therefore appeared

to be isomers of M_2BeH_4 molecules. Hereafter these isomers are denoted as I, II, and III, for C_{2v} compact, D_{2d}, and C_{2v} hexagonal, respectively; the equilibrium geometrical configurations are shown in Fig. 4 and the parameters are displayed in Tables 8−10.

Table 8. Properties of M_2BeH_4 (M = Li, Na) molecules (C_{2v}, compact structure)

Property	Li_2BeH_4		Na_2BeH_4	
	DFT/B3PW91	MP2	DFT/B3PW91	MP2
$R_{e1}(Be_1-H_2)$	1.530	1.525	1.533	1.528
$R_{e2}(Be_1-H_4)$	1.413	1.406	1.430	1.422
$R_{e3}(M_7-H_2)$	1.865	1.863	2.252	2.247
$R_{e4}(M_7-H_5)$	1.822	1.82	2.126	2.125
$\alpha_e(H_3-M_6-H_4)$	78.0	77.8	66.5	66.2
$\beta_e(H_3-M_7-H_2)$	70.4	70.2	60.7	60.3
$\gamma_e(H_3-Be_1-H_4)$	104.1	104.2	108.2	108.1
$\delta_e(H_3-Be_1-H_2)$	89.3	89.2	95.8	95.2
$-E$	32.20966	32.03993	341.66059	341.04435
ω_1 (A_1)	1702 (1.52)	1743 (1.68)	1622 (3.16)	1663 (3.47)
ω_2 (A_1)	1409 (8.62)	1448 (8.67)	1338 (11.2)	1371 (11.9)
ω_3 (A_1)	1015 (4.97)	1061 (8.68)	994 (1.67)	1046 (2.43)
ω_4 (A_1)	1004 (8.11)	1043 (6.67)	936 (7.75)	997 (10.0)
ω_5 (A_1)	639 (1.31)	651 (1.47)	387 (1.66)	397 (1.75)
ω_6 (A_1)	275 (0.23)	282 (0.70)	132 (0.41)	136 (0.40)
ω_7 (A_2)	1038 (0)	1072 (0)	961 (0)	999 (0)
ω_8 (A_2)	476 (0)	492 (0)	333 (0)	357 (0)
ω_9 (B_1)	1772 (13.7)	1810 (14.7)	1650 (17.3)	1696 (19.4)
ω_{10} (B_1)	1106 (9.36)	1146 (10.6)	1038 (6.60)	1094 (8.89)
ω_{11} (B_1)	741 (0.45)	755 (0.42)	643 (0.05)	675 (0.08)
ω_{12} (B_1)	674 (5.41)	686 (5.93)	459 (4.73)	466 (4.98)
ω_{13} (B_2)	1259 (13.8)	1282 (14.5)	1207 (17.5)	1230 (18.4)
ω_{14} (B_2)	894 (5.76)	934 (7.20)	845 (7.37)	890 (9.44)
ω_{15} (B_2)	384 (0.02)	389 (0.24)	270 (0.03)	283 (0.03)
μ_e	5.6	5.8	7.7	8.2

The binding in the polyhedral and two−cycled structures may be considered through an attachment of two M atoms to a slightly distorted tetrahedral BeH_4 moiety. In the first isomer , there are two types of Be−H bonds with internuclear separations $R_{e1}(Be-H) \approx 1.53$ Å and $R_{e2}(Be-H) \approx 1.42$ Å; the average of these two values, 1.47 Å, is very close to the distance $R_e(Be-H)$ in the D_{2d} isomer. The averaged valence angle H−Be−H in BeH_4 fragment of the polyhedral isomers is about 109° that is almost equal to the tetrahedral angle. In the D_{2d} isomer, the angle H−Be−H is 104° (Li_2BeH_4) and 110° (Na_2BeH_4) that is also close to the tetrahedral angle. The hexagonal molecule may be considered through a combination of BeH_3^- and M_2H^+ subunits. The geometrical parameters, the bridge Be−H bond lengths (~1.42 Å) and valence

angle β_e (H−Be−H) ≈ 117°, of the hexagonal M_2BeH_4 molecules are similar to the respective parameters in free BeH_3^- ion as well as in cyclic $MBeH_3$ molecules.

Table 9. Properties of M_2BeH_4 (M = Li, Na) molecules (D_{2d})

Property	Li_2BeH_4		Na_2BeH_4	
	DFT/B3PW91	MP2	DFT/B3PW91	MP2
R_{e1}(Be$_1$−H$_2$)	1.471	1.464	1.477	1.470
R_{e2}(M$_7$−H$_2$)	1.718	1.715	2.060	2.060
α_e(H$_2$−M$_7$−H$_5$)	84.9	84.5	72.3	71.5
β_e(H$_2$−Be$_1$−H$_5$)	104.1	103.9	110.8	109.9
$-E$	32.20384	32.03404	341.65577	341.03837
$\Delta_r E_{iso}$(I−II)	15.3	15.5	12.6	15.7
ω_1 (A_1)	1537 (0)	1573 (0)	1497(0)	1533 (0)
ω_2 (A_1)	1221 (0)	1261 (0)	1122(0)	1165 (0)
ω_3 (A_1)	457 (0)	464 (0)	222(0)	225 (0)
ω_4 (B_1)	733 (0)	758 (0)	769(0)	795 (0)
ω_5 (B_2)	1520 (17.9)	1554 (19.2)	1440 (24.2)	1474 (26.2)
ω_6 (B_2)	1213 (21.3)	1259 (24.2)	1118 (13.2)	1160 (15.6)
ω_7 (B_2)	701 (4.43)	717 (4.5)	506 (3.65)	514 (3.82)
ω_8 (E)	1436 (30.0)	1464 (32.5)	1408 (35.5)	1441 (39.0)
ω_9 (E)	1107 (7.0)	1144 (8.98)	957 (7.86)	996 (11.32)
ω_{10} (E)	706 (2.90)	729 (3.58)	596 (1.42)	613 (1.76)
ω_{11} (E)	101 (7.58)	114 (7.84)	26 (7.36)	21 (8.08)

Note: $\Delta_r E_{iso}$(I−II) is the energy of isomerization reaction M_2BeH_4 (I, $C_{2v, comp}$) = M_2BeH_4 (II, D_{2d}), $\Delta_r E_{iso}$(I−II) = E(II) − E(I), in kJ·mol^{-1}
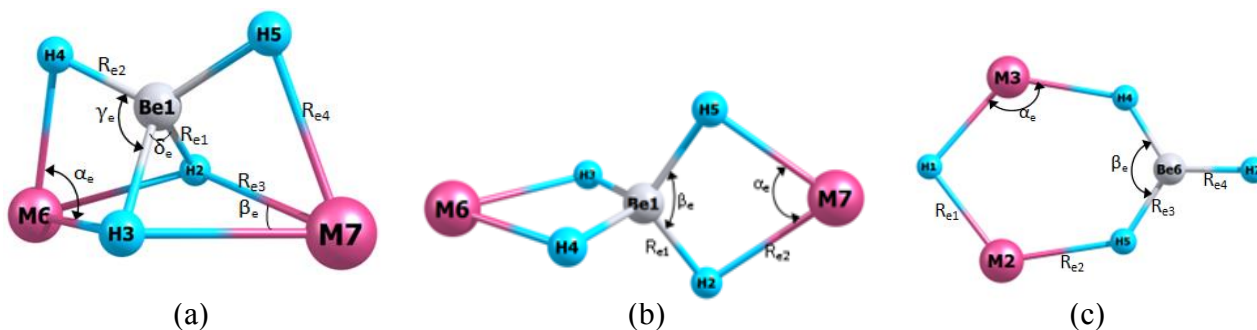
Figure 4. Equilibrium geometrical configurations of M_2BeH_4 isomers: (a) I, polyhedral (C_{2v}); (b) II, two−cycled (D_{2d}); (c) III, hexagonal (C_{2v})

The IR spectra of three isomers of Li_2BeH_4 and Na_2BeH_4 molecules are presented in Fig. 5. By comparing IR spectra of Li_2BeH_4 and Na_2BeH_4 molecules, alike features may be observed for the isomers of the same symmetry. For the polyhedral isomer I, the bands of high intensity are at 1259 cm^{-1}, 1772 cm^{-1} (Li_2BeH_4) and 1207 cm^{-1}, and 1650 cm^{-1} (Na_2BeH_4) correspond to H−Be−H asymmetrical stretching vibrations of BeH_4 moiety. For the two−cycled D_{2d} isomer,

similar H−Be−H asymmetrical stretching vibrations of BeH_4 moiety are observed at 1436 cm^{-1}, 1520 cm^{-1} (Li_2BeH_4) and 1408 cm^{-1}, 1440 cm^{-1} (Na_2BeH_4). The most intensive band in spectrum of Li_2BeH_4 D_{2d} is seen at 1213 cm^{-1} and corresponds to the H−Li−H asymmetrical stretching mode, in Na_2BeH_4 D_{2d} the similar vibration is observed at 1118 cm^{-1}. For the hexagonal isomer the most intense bands appear at 1764 cm^{-1} (Li_2BeH_4) and 1742 cm^{-1} (Na_2BeH_4) and are characterized by stretching modes of the BeH_3 fragment. Other similarities may be noted between two hexagonal species as wagging vibrations at 444 cm^{-1} Li−H−Li, 794 cm^{-1} H−Be−H (Li_2BeH_4) and 344 cm^{-1} Na−H−Na, 797 cm^{-1} H−Be−H (Na_2BeH_4). The vibration of highest frequency at about 2000 cm^{-1}, both for Li_2BeH_4 and Na_2BeH_4, corresponds to the terminal bond Be−H stretching mode, that is the highest frequency correlates with the shortest bond length R_e(Be−H) = 1.36 Å.

Table 10. Properties of M_2BeH_4 (M = Li, Na) molecules (C_{2v}, hexagonal structure)

Property	Li_2BeH_4		Na_2BeH_4	
	DFT/B3PW91	MP2	DFT/B3PW91	MP2
$R_{e1}(M_2-H_1)$	1.705	1.700	2.050	2.049
$R_{e2}(M_2-H_5)$	1.704	1.696	2.046	2.046
$R_{e3}(Be_6-H_5)$	1.426	1.421	1.425	1.418
$R_{e4}(Be_6-H_7)$	1.357	1.352	1.365	1.360
$\alpha_e(H_1-M_3-H_4)$	127.7	126.7	119.3	118.1
$\beta_e(H_4-Be_6-H_5)$	118.2	116.7	117.1	116.4
$-E$	32.19484	32.028467	341.65258	341.03774
$\Delta_r E_{iso}$(I–III)	38.9	30.1	21.0	17.4
μ_e	4.5	4.6	5.4	5.5
ω_1 (A_1)	1988 (7.94)	2033 (8.62)	1946 (9.37)	1988 (10.1)
ω_2 (A_1)	1764 (13.4)	1817 (10.5)	1754 (8.74)	1806 (9.26)
ω_3 (A_1)	1090 (2.29)	1130 (2.20)	971 (1.83)	1011 (2.33)
ω_4 (A_1)	1045 (11.6)	1067 (12.5)	857 (12.8)	866 (13.6)
ω_5 (A_1)	429 (0.61)	446 (0.57)	325 (0.88)	333 (0.92)
ω_6 (A_1)	382 (0.33)	386 (0.40)	174 (0.14)	176 (0.16)
ω_7 (A_2)	234 (0)	252 (0)	180 (0)	185 (0)
ω_8 (B_1)	1763 (9.07)	1808 (14.4)	1742 (14.8)	1791 (16.2)
ω_9 (B_1)	1205 (11.1)	1243 (12.1)	975 (12.8)	1005 (13.9)
ω_{10} (B_1)	1015 (3.19)	1042 (4.05)	917 (3.44)	949 (3.99)
ω_{11} (B_1)	553 (1.05)	569 (1.07)	435 (0.10)	442 (0.09)
ω_{12} (B_1)	150 (1.61)	175 (2.04)	35 (1.55)	64 (1.69)
ω_{13} (B_2)	794 (11.6)	835 (12.3)	797 (10.6)	839 (11.7)
ω_{14} (B_2)	445 (5.83)	454 (6.52)	344 (8.17)	345 (9.28)
ω_{15} (B_2)	149 (1.95)	153 (1.54)	122 (1.27)	113 (1.29)
μ_e	4.5	4.6	5.4	5.5

Note: $\Delta_r E_{iso}$(I–III) is the energy of isomerization reaction M_2BeH_4 (I, $C_{2v, comp}$) = M_2BeH_4 (III, $C_{2v, hex}$), $\Delta_r E_{iso}$(I–III) = E(III) − E(I), in kJ·mol^{-1}
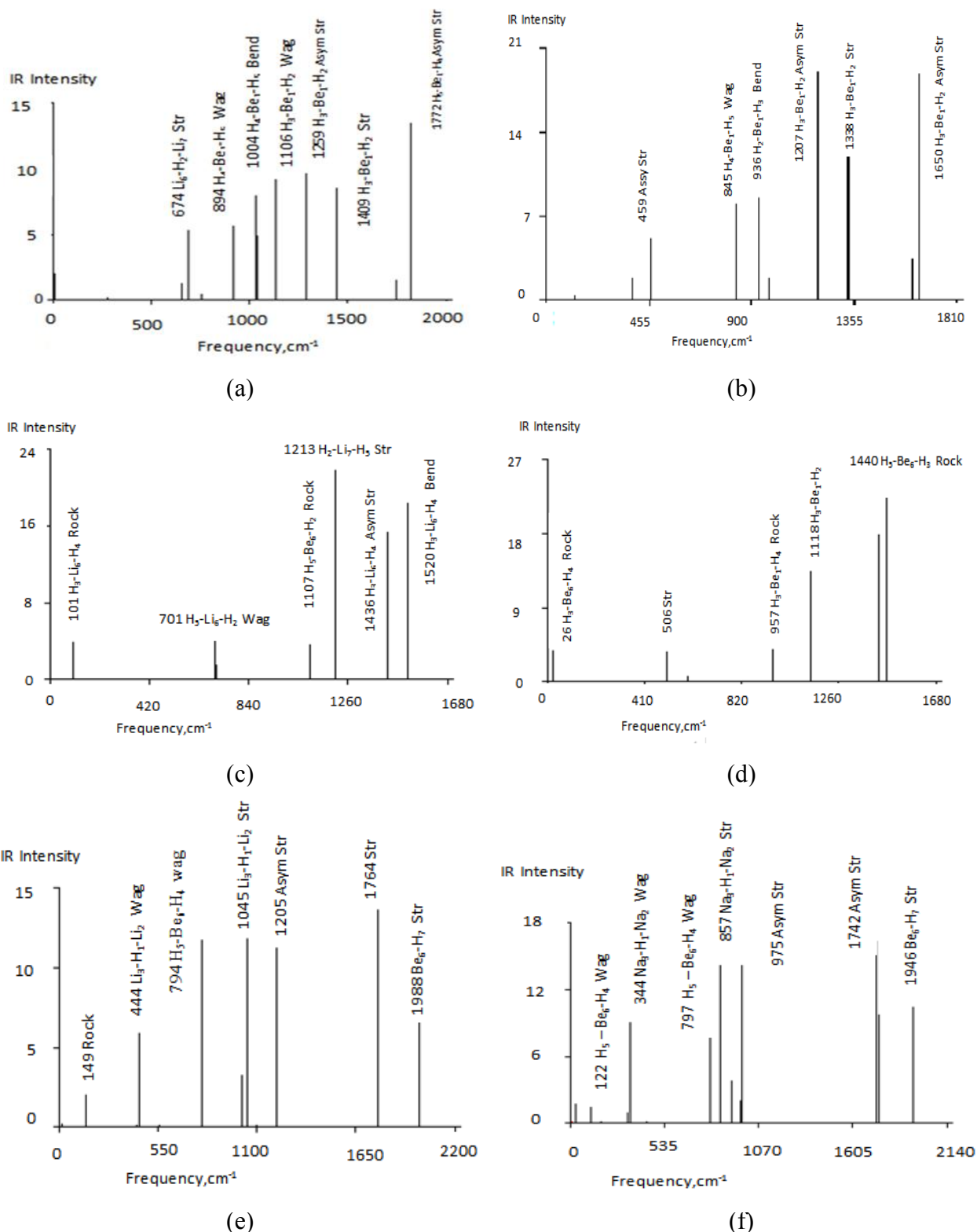
Figure 5. IR spectra of complex hydrides M₂BeH₄ (M = Li, Na) calculated by DFT/B3PW91: (a) Li₂BeH₄ (*C*₂ᵥ, compact); (b) Na₂BeH₄ (*C*₂ᵥ, compact); (c) Li₂BeH₄ (*D*₂d); (d) Na₂BeH₄ (*D*₂d); (e) Li₂BeH₄ (*C*₂ᵥ, hexagonal); (f) Na₂BeH₄ (*C*₂ᵥ, hexagonal)

The relative energies $\Delta_r E_{iso}$ of the isomers II and III regarding I given in Tables 9 and 10 were

calculated for the following isomerisation reactions:

$$M_2BeH_4(I, C_{2v, comp}) = M_2BeH_4(II, D_{2d}) \qquad (7)$$

$$M_2BeH_4(I, C_{2v, comp}) = M_2BeH_4(III, C_{2v, hex}). \qquad (8)$$
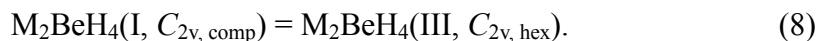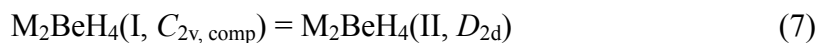
The values of $\Delta_r E_{iso}$ are positive: for reaction 7, 15.5 kJ mol^{-1} (Li$_2$BeH$_4$), 15.7 kJ mol^{-1} (Na$_2$BeH$_4$), and for reaction 8, 30.1 kJ mol^{-1} (Li$_2$BeH$_4$), 17.4 kJ mol^{-1} (Na$_2$BeH$_4$) according to MP2 calculations. Therefore among three isomers, I, II, and III, the first one has the lowest energy, followed by D_{2d}, and the hexagonal: $E(I) < E(II) < E(III)$ for both molecules. The energy difference between isomers II and III is 14.6 kJ mol^{-1} (Li$_2$BeH$_4$), and 1.7 kJ mol^{-1} (Na$_2$BeH$_4$) in favour of D_{2d}, thus worth to note the isomers II and III of the Na$_2$BeH$_4$ molecule are comparable by energy.

To evaluate the relative concentration of the isomers in the equilibrium vapour, the thermodynamic approach was applied. The following equation was used:

$$\Delta_r H°(0) = T\Delta_r \Phi°(T) - RT \ln\left(\frac{p_A}{p_B}\right) \qquad (9)$$

where $\Delta_r H°(0)$ is the enthalpy of isomerisation of the reaction; T is absolute temperature; $\Delta_r \Phi°(T)$ is the reduced Gibbs energy of the reaction, $\Phi°(T) = -[H°(T)-H°(0)-TS°(T)]/T$; p_A/p_B is the pressure ratio between two isomers, that is p_{II}/p_I for reaction 7 and p_{III}/p_I for reaction 8. The values of $\Delta_r H°(0)$ were calculated using isomerization energies $\Delta_r E_{iso}$ and the ZPVE corrections $\Delta_r \varepsilon$ by Eqs. (3) and (4). The relative concentrations p_A/p_B have been calculated for the temperature range between 500 and 2000 K; the plots are shown in Fig. 6. The graphs show that the relative concentrations of the isomers II and III increase with temperature increase for both molecules, for Li$_2$BeH$_4$ the growth is slow compared to Na$_2$BeH$_4$. At 1000 K for Li$_2$BeH$_4$ and Na$_2$BeH$_4$ the values of p_{II}/p_I are equal to 0.6 and 5.2, respectively, while the ratios p_{III}/p_I are 2.5 and 30, respectively. Therefore the isomer I of Li$_2$BeH$_4$ molecule is more abundant at moderate temperatures, but at higher temperatures its concentration decreases significantly. For Na$_2$BeH$_4$ the hexagonal isomer is much more abundant compared to either isomers I and II. The fraction of each isomer of Na$_2$BeH$_4$ was estimated as $x_i = p_i/(p_I + p_{II} + p_{III})$ where i stands for I, II, or III, the results for two selected temperatures are given in Table 11. Thus it can be concluded that the hexagonal isomer of Na$_2$BeH$_4$ is predominant in a broad temperature range and its concentration is increasing with temperature raise.

(a)   (b)
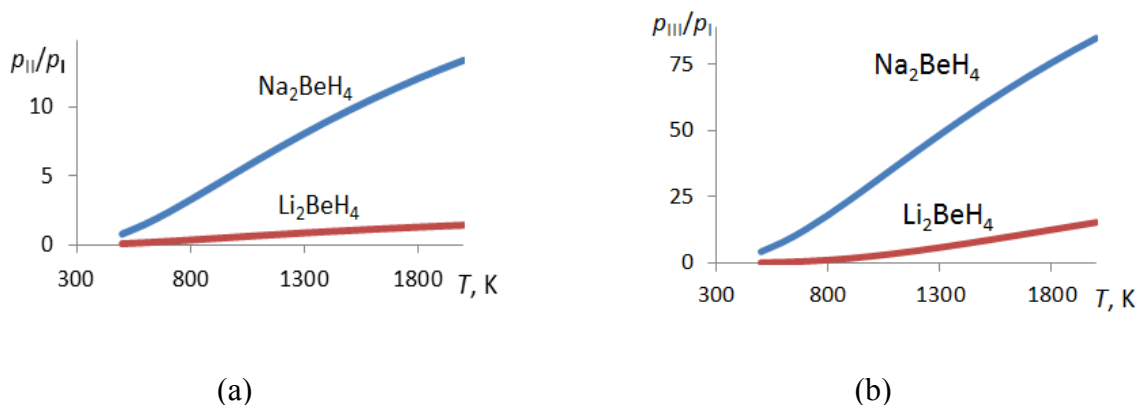
Figure 6. Relative abundance pA/pB versus temperature for three isomers of complex hydrides M_2BeH_4 by MP2 method: (a) $p_{II}(D_{2d})/p_I(C_{2v}, comp)$; (b) $p_{III}(C_{2v}, hex)/ p_I(C_{2v}, comp)$

Table 11. The fraction xi of isomers I, II, and III in equilibrium vapour of Na_2BeH_4

T, K	x_I	x_{II}	x_{III}
500	0.26	0.22	0.52
1000	0.03	0.14	0.83

2.4 *Thermodynamic Properties of Complex Hydrides*

2.4.1. *The Enthalpies of Dissociation Reactions and Enthalpies of Formation of Molecules*

Different dissociation reactions of the complex hydrides $MBeH_3$ and M_2BeH_4 have been examined; for the latter the polyhedral isomer of C_{2v} symmetry was considered as lowest by energy. The calculated energies and enthalpies of gas−phase reactions are represented in Tables 12 and 13; the results obtained by DFT/B3PW91 and MP2 methods. Two types of dissociation reactions of complex hydrides, $MBeH_3$ and M_2BeH_4 were considered: a partial dissociation and complete reduction of the hydride with hydrogen gas release. The values of $\Delta_r H°(0)$ show that all reactions proceed with the absorption of energy (endothermic). The partial dissociation of both penta− and heptaatomic hydrides requires much less energy than reaction with hydrogen formation. The most energy consuming reactions are those with H_2 evolving (reactions 2 for $MBeH_3$ and 6, 7 for M_2BeH_4) and dissociation into ionic subunits M_2H^+ and BeH_3^- (reactions 8).

The enthalpies of formation $\Delta_f H°(0)$ of the complex hydrides were calculated through the enthalpies of the reactions and enthalpies of formation of the gaseous products, Li, Na, H_2, LiH, NaH (Gurvich *et al.*, 1992) and BeH_2 (NIST). The enthalpies of formation of M_2H_2 molecules involved in reactions 5 were obtained through the enthalpies of dimerization reactions (Table 5),

18

the averaged values of $\Delta_f H°(0)$ between DFT/B3PW91 and MP2 methods were accepted: 90 ± 10 kJ·mol^{-1} (Li_2H_2) and 139 ± 10 kJ·mol^{-1} (Na_2H_2). The enthalpies of formation of the penta− and heptaatomic hydrides are presented in the far right column in Tables 12, 13. The enthalpies of formation of $MBeH_3$ molecules are accepted as the averaged values found through the enthalpies of reactions 1 and 2; similarly for M_2BeH_4 through reactions 3−7. Uncertainties were estimated as half−differences between maximum and minimum magnitudes. The accepted values of $\Delta_f H°(0)$ are gathered in Table 14.

Table 12. The energies and enthalpies of gas−phase dissociation reactions, and enthalpies of formation of gaseous complex hydrides $LiBeH_3$ and Li_2BeH_4; all values are given in kJ mol^{-1}

No	Reaction	Method	$\Delta_r E$	$\Delta_r \varepsilon$	$\Delta_r H°(0)$	$\Delta_f H°(0)$
1	$LiBeH_3 = LiH + BeH_2$	DFT/B3PW91	197.77	−16.57	181.20	83.76
		MP2	198.81	−17.67	181.14	83.82
2	$LiBeH_3 = Li + Be + 3/2H_2$	DFT/B3PW91	382.73	−19.28	363.49	114.00
		MP2	360.87	−19.90	340.98	136.51
3	$Li_2BeH_4 = LiBeH_3 + LiH$	DFT/B3PW91	210.31	−61.09	149.22	73.98
		MP2	211.54	−62.74	148.79	74.47
4	$Li_2BeH_4 = 2LiH + BeH_2$	DFT/B3PW91	408.08	−35.38	372.70	31.70
		MP2	410.34	−36.96	373.38	31.02
5	$Li_2BeH_4 = Li_2H_2 + BeH_2$	DFT/B3PW91	207.0	−21.09	185.91	29.60
		MP2	202.43	−22.26	180.2	35.30
6	$Li_2BeH_4 = 2LiH + Be + H_2$	DFT/B3PW91	589.47	−42.90	546.57	52.06
		MP2	580.64	−44.14	536.50	62.13
7	$Li_2BeH_4 = 2Li + Be + 2H_2$	DFT/B3PW91	596.61	−33.21	563.40	71.82
		MP2	564.18	−34.23	529.95	105.29
8	$Li_2BeH_4 = Li_2H^+ + BeH_3^-$	DFT/B3PW91	603.02	−23.96	579.67	
		MP2	605.02	−23.64	581.38	

Table 13. The energies and enthalpies of gas−phase dissociation reactions, and enthalpies of formation of gaseous complex hydrides $NaBeH_3$ and Na_2BeH_4; all values are given in kJ mol^{-1}

No	Reaction	Method	$\Delta_r E$	$\Delta_r \varepsilon$	$\Delta_r H°(0)$	$\Delta_f H°(0)$
1	$NaBeH_3 = NaH + BeH_2$	DFT/B3PW91	178.71	−14.22	164.49	103.83
		MP2	186.70	−15.59	171.31	97.01
2	$NaBeH_3 = Na + Be + 3/2H_2$	DFT/B3PW91	311.65	−15.58	296.07	131.44
		MP2	320.36	−15.73	304.63	151.34
3	$Na_2BeH_4 = NaBeH_3 + NaH$	DFT/B3PW91	167.02	−55.09	111.94	134.69
		MP2	176.20	−57.50	118.69	121.12
4	$Na_2BeH_4 = 2NaH + BeH_2$	DFT/B3PW91	345.74	−28.63	317.11	94.01
		MP2	362.90	−30.95	331.94	79.18
5	$Na_2BeH_4 = Na_2H_2 + BeH_2$	DFT/B3PW91	196.74	−19.59	177.14	87.50
		MP2	199.66	−20.75	178.90	85.70
6	$Na_2BeH_4 = 2NaH + Be + H_2$	DFT/B3PW91	527.13	−36.15	490.98	114.37
		MP2	533.19	−38.14	495.05	110.30
7	$Na_2BeH_4 = 2Na + Be + 2H_2$	DFT/B3PW91	430.22	−23.81	406.41	128.87
		MP2	403.86	−25.30	378.57	156.71
8	$Na_2BeH_4 = Na_2H^+ + BeH_3^-$	DFT/B3PW91	499.40	−18.58	480.00	
		MP2	497.94	−17.95	480.00	

Table 14. Accepted enthalpies of formation (in kJ mol⁻¹) of gaseous complex hydrides MBeH$_3$ and M$_2$BeH$_4$ (M = Li, Na)

Hydride	$\Delta_f H°(0)$	Hydride	$\Delta_f H°(0)$
LiBeH$_3$	105 ± 26	NaBeH$_3$	121 ± 27
Li$_2$BeH$_4$	63 ± 37	Na$_2$BeH$_4$	117 ± 39

Stability of the gaseous complex hydrides MBeH$_3$ and M$_2$BeH$_4$ regarding heterophase decomposition with hydrogen release were also considered. The enthalpies of the heterophase reactions were calculated and given in Table 15. The required enthalpies of formation of Be, LiH, NaH, Li, Na in condensed phase were taken from Gurvich *et al*., (1992). In the heterophase reactions considered, beryllium is in solid state, the alkali metal hydrides are in gas−phase (reactions 1, 4) or in condensed phase (reactions 2, 5); complete decomposition is described by reactions 3, 6. The results show that the reactions in which gaseous MH are among the products are endothermic, while the rest reactions are exothermic; the biggest energy being released in reactions 2 and 5 with MH$_{(c)}$.

2.4.2 Thermal Stability of the Complex Hydrides and Thermodynamic Favourability of the Reactions

The thermodynamic stability of the complex hydrides MBeH$_3$ and M$_2$BeH$_4$ was examined through Gibbs free energies for heterophase reactions shown in Table 15. The temperature dependences of $\Delta_r G°(T)$ are presented in Figs. 7−9. For the reactions in which MH is in gaseous phase, $\Delta_r G°(T)$ are negative at moderate and elevated temperatures (Fig. 7); the decomposition reactions are thermodynamically favoured at temperatures above 350 K (NaBeH$_3$), 500 K (LiBeH$_3$), 800 K (Na$_2$BeH$_4$) and 1000 K (Li$_2$BeH$_4$). Thus the MBeH$_3$ hydrides appeared to be less stable thermodynamically than M$_2$BeH$_4$ and Na−containing hydrides are less stable compared to Li−hydrides.

For reactions in which both MH and Be are in condensed phase (Fig. 8) the values of $\Delta_r G°(T)$ are negative for whole temperature range considered. The Na−containing hydrides are slightly more stable than Li−hydrides as the values of $\Delta_r G°(T)$ for the former are less negative. The inflections on the curves correspond to phase change transition of the products, namely the melting points of LiH$_{(c)}$ and NaH$_{(c)}$ at 965 K and 911 K respectively (Gurvich *et al*., 1992). The Gibbs free energy for the decomposition reaction of MBeH$_3$ increases with temperature raise, while for M$_2$BeH$_4$ hydrides the values of $\Delta_r G°$ pass through maximum at temperatures of the phase transitions. Here the entropy has an impact on $\Delta_r G°(T)$: as a jump of entropy at phase transition of MH$_{(c)}$

occurs hence the contribution of entropy factor $T\Delta_r S$ increases with temperature raise.

Table 15. The enthalpies of heterophase dissociation reactions of gaseous hydrides MBeH$_3$ and M$_2$BeH$_4$

No	Reaction	$\Delta_r H°(0)$, kJ mol^{-1}	
		M = Li	M = Na
1	$MBeH_3 = MH_{(g)} + Be_{(c)} + H_{2(g)}$	34	22
2	$MBeH_3 = MH_{(c)} + Be_{(c)} + H_{2(g)}$	−191	−173
3	$MBeH_3 = M_{(c)} + Be_{(c)} + 3/2H_{2(g)}$	−105	−121
4	$M_2BeH_4 = 2MH_{(g)} + Be_{(c)} + H_{2(g)})$	220	172
5	$M_2BeH_4 = 2MH_{(c)} + Be_{(c)} + H_{2(g)}$	−234	−221
6	$M_2BeH_4 = 2M_{(c)} + Be_{(c)} + 2H_{2(g)}$	−63	−117
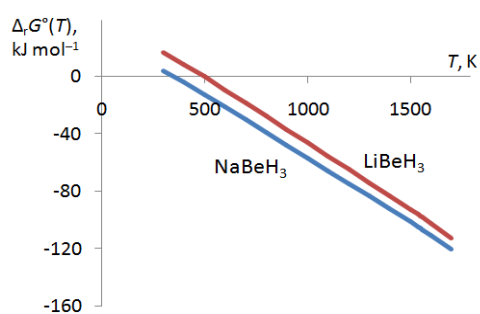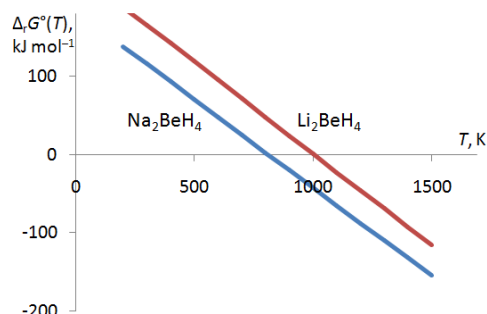
(a)   (b)

Figure 7. Gibbs free energy $\Delta_r G°(T)$ against temperature for heterophase decomposition reactions of complex hydrides MBeH$_3$ and M$_2$BeH$_4$: (a) MBeH$_3$(g) = MH(g) + Be(c) + H$_2$(g); (b) M$_2$BeH$_4$(g) = 2MH(g) + Be(c) + H$_2$(g)
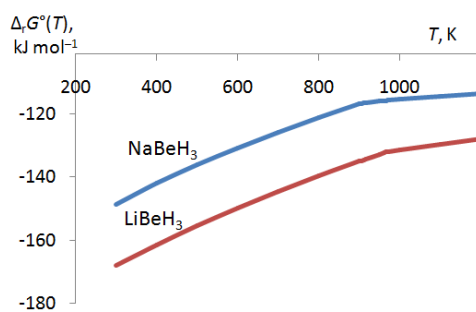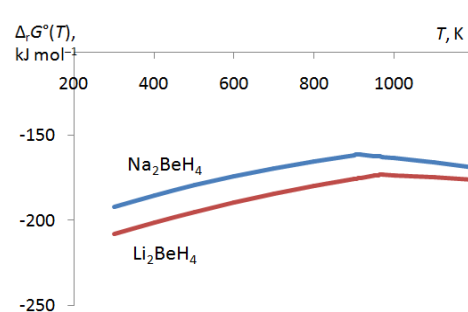
(a)   (b)

Figure 8. Gibbs free energy $\Delta_r G°(T)$ against temperature for heterophase decomposition reactions of complex hydrides MBeH$_3$ and M$_2$BeH$_4$: (a) MBeH$_3$(g) = MH(c) + Be(c) + H$_2$(g); (b) M$_2$BeH$_4$(g) = 2MH(c) + Be(c) + H$_2$(g)

For the reactions with complete dissociation into alkaline metal and beryllium in condensed phase (Fig. 9) the Gibbs free energies are negative in the temperature range considered and decreasing with temperature increase, this indicates that the decomposition processes are

21

spontaneous. In contrast to previous case (Fig. 8), the Na−containing hydrides are less stable than Li−hydrides as the values of $\Delta_r G°(T)$ are less negative for the latter.

For different channels of dissociation of the hydrides, a correlation between $\Delta_r G°(T)$ and $\Delta_r H°(0)$ values may be noted: the lower is the enthalpy of the reaction the more negative are $\Delta_r G°(T)$ and hence the more favourable the decomposition process. For instance, for the reactions with gaseous alkali hydrides MH the enthalpies $\Delta_r H°(0)$ are positive, ~20–30 kJ mol^{-1} (MBeH$_3$) and ~170–220 kJ mol^{-1} (M$_2$BeH$_4$); then the Gibbs free energies are positive at low and moderate temperatures and turn negative at certain temperatures said (Fig. 7). This implies that the reversibility of the reactions is able to be attained. For other heterogeneous reactions the $\Delta_r H°(0)$ values are negative, the Gibbs free energies are negative (Figs. 8, 9) that is the decomposition of the hydrides, both MBeH$_3$ and M$_2$BeH$_4$, is spontaneous in the whole temperature range considered. The reaction with Li/Na and Be in condensed phase the reversibility may be achieved by pressure increase (Le Châtelier's principle). The reversibility of the decomposition reactions of hydrides is one of the requirements for hydrogen storage materials.
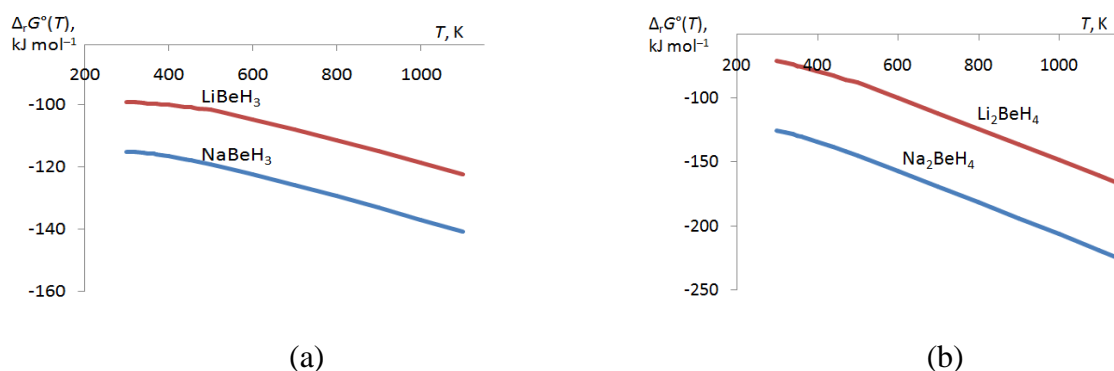
Figure 9. Gibbs free energy $\Delta_r G°(T)$ against temperature for heterophase decomposition reactions of complex hydrides MBeH$_3$ and M$_2$BeH$_4$: (a) MBeH$_3$(g) = M(c) + Be(c) + 3/2H$_2$(g); (b) M$_2$BeH$_4$(g) = 2M(c) + Be(c) + 2H$_2$(g)

2.5 Conclusion

The geometrical parameters, vibrational spectra and thermodynamic properties of the complex hydrides MBeH$_3$ and M$_2$BeH$_4$ (M = Li, Na) and subunits have been determined using DFT/B3PW91 and MP2 methods. The results obtained by both methods are in a good agreement with the reference data available for subunits MH, BeH$_2$, M$_2$H$_2$. The enthalpies of different gas−phase dissociation reactions were computed; the enthalpies of formation of the complex hydrides were found. The Gibbs free energies $\Delta_r G°(T)$ of heterophase decomposition of MBeH$_3$

and M_2BeH_4 with hydrogen release were analyzed. It was shown that the reactions the products of which were gaseous alkaline metals and solid beryllium may be reversible at moderate temperatures. The decomposition reaction of $MBeH_3$ and M_2BeH_4, giving $M_{(c)}$, $Be_{(c)}$, H_2 as products, were found to spontaneous at a broad temperature range; the reversibility of the reactions may be attained if certain conditions are provided. The complex hydrides $MBeH_3$ and M_2BeH_4 (M = Na or Li) may be considered as promising candidates for hydrogen storage applications as they showed the feasibility of hydrogen gas production.

CHAPTER THREE

Gaseous Metal Hydrides $MMgH_3$ and M_2MgH_4 (M= Li, Na): Quantum Chemical Study of Structure, Vibrational Spectra and Thermodynamic Properties

Abstract

The complex hydrides $MMgH_3$ and M_2MgH_4 (M = Li, Na) have been studied using DFT, MP2 methods with basis set 6−311++G(d,p). The equilibrium geometrical structure, vibrational spectra and thermodynamic properties have been calculated. For pentaatomic $MMgH_3$ molecules, two isomeric forms were found: the cyclic (C_{2v}) and linear ($C_{\infty v}$), the latter had higher energy by ~130 $kJ \cdot mol^{-1}$. Three isomers of M_2MgH_4 hydrides were proved to exist and their equilibrium geometrical configurations were found as follows: two−cycled (D_{2d}), polyhedral (C_{2v}) and hexagonal (C_{2v}). Among these three, the hexagonal isomer possessed the lowest energy being predominant in saturated vapour. The enthalpies of formation $\Delta_f H°(0)$ of the hydrides in gaseous phase were determined (in $kJ \cdot mol^{-1}$): 114 ± 13 ($LiMgH_3$), 113 ±12 (Li_2MgH_4), 162 ± 11 ($NaMgH_3$), and 175 ± 26 (Na_2MgH_4). Gas phase and heterophase decomposition of the hydrides was examined applying a thermodynamic approach.

3.1 Introduction

Hydrogen, as the most available element in the universe, is very essential as energy source. It is also clean and forms water as a harmless byproduct during the use. But one of its biggest drawbacks is storage (Vajeeston *et al*., 2008). However, the possibility of using hydrogen as a reliable energy carrier has recently motivated intense research in hydrogen−based energy systems (Amsler *et al*., 2012) and therefore, this motivated many researches to be done for alkali complex hydrides mainly from the viewpoint of kinetics (Zidan *et al*., 1999; Zaluski *et al*., 1999; Gross, 2000; Bogdanović and Schwickardi 1997; Sun, 2002; Meisner, 2002; Sandrock *et al*., 2002; Morioka *et al*., 2003). Despite the researches which have been done, in recent overview by (Riis *et al*., 2005) on the three principal forms of hydrogen storage (gas, liquid, and solid) the technology gaps and research and development priorities were focused.

A number of challenges remain and new media are needed that are capable of safely storing hydrogen with high gravimetric and volumetric densities. Metal hydrides and complex metal hydrides offer some hope of overcoming these challenges (Graetz, 2012). The complex hydrides Li_2MH_5 (M = B or Al) were previously studied theoretically and it was found that these materials

are stable at low temperatures and confirmed to be potential for hydrogen storage purposes (Tsere *et al.*, 2015).

It was reported that for the purpose of decreasing the hydrogen desorption temperatures, there is a need of systematic understanding of the thermodynamical stabilities of these hydrides. For instance, the stabilities of alkali borohydrides have been studied by first−principles calculation (Nakamori *et al.*, 2006). Palumbo *et al.* (2007) also investigated the thermodynamic stability of alanate magnesium hydrides in order to see its suitability for commercial applications in automotive. Moreover, the dehydrogenation behaviour of the ternary hydride $NaMgH_3$ was investigated by temperature programmed desorption (Reardon *et al.*, 2013).

The desorption mechanism of the complex metal hydrides such as sodium magnesium hydride $NaMgH_3$ to release hydrogen gas was described by (Ikeda *et al.*, 2005) to proceed in the following two channels:

$$NaMgH_3 \rightarrow NaH + Mg + H_2 \tag{10}$$
$$NaMgH_3 \rightarrow Na + Mg + 3/2H_2 \tag{11}$$

This study, therefore aimed at theoretical investigation of the properties of complex hydrides $MMgH_3$ and M_2MgH_4 (M = Li, Na) in gaseous state; as these species are expected to be potential candidate for hydrogen storage purposes. The content of hydrogen is 8.8% ($LiMgH_3$), 6.0% ($NaMgH_3$), 9.5% (Li_2MgH_4), and 5.4% (Na_2MgH_4). The geometrical parameters, vibrational spectra and thermodynamic properties of the complex hydrides $MBeH_3$ and M_2BeH_4 (M = Li, Na) have been determined using DFT/B3PW91 and MP2 methods in our previous work reported in Chapter twa and found that these hydrides may be are promising materials for hydrogen storage application. In present work we continue the similar investigation of the other group of complex hydrides: $MMgH_3$ and M_2MgH_4 (M = Li, Na).

3.2 Computational Details

The methodology of calculations was described in Chapter two. In this work, two quantum chemical approaches, DFT/B3PW91 and MP2 with basis set 6−311++G(d,p) were employed to optimize the geometrical parameters and calculate vibrational frequencies of the complex hydrides and their subunits. Different dissociation channels of the hydrides were considered; the

enthalpies and Gibbs energies of reactions were computed. The details of calculations and equations used are specified in Chapter two.

3.3 Results and Discussion

3.3.1 *Subunits of Complex Hydrides*

Among possible dissociation products of the complex hydrides $MMgH_3$ and M_2MgH_4 (M = Li, Na) the following species were considered: diatomic molecules, H_2, LiH and NaH, triatomic molecule MgH_2 and ions Li_2H^+ and Na_2H^+ and tetraatomic molecules Li_2H_2 and Na_2H_2 and MgH_3^- ion. The diatomic species as well as triatomic ions and the dimer molecule were given in Chapter two.

Triatomic molecule MgH₂

The characteristics of the MgH_2 molecule are summarized in Table 16 and its structure displayed in Fig. 10 a. The corresponding values obtained through the two methods are generally in agreement with each other and reference data (Jacox, 1994). The value of equilibrium internuclear distance by DFT exceeded that of MP2 by 0.006 Å, while the valence asymmetric frequency ω_2 is overrated by 2.9% (DFT) and 6.0% (MP2) respectively compared to experimental magnitude. For the frequency ω_3 is exceeded by 3.6% (DFT) and 1.1% (MP2) in respect to the experimental value. The results show that for ω_2 the DFT is more close to the experimental data while for ω_3 the MP2 is more close to the experimental data.

Table 16. Properties of triatomic molecule MgH₂

Property	DFT/B3PW91	MP2	Expt
Re(Mg−H)	1.709	1.703	
$-E$	201.21061	200.90787	
$\omega_1 (\textstyle\sum_g^+)$	1593 (0)	1645 (0)	
$\omega_2 (\textstyle\sum_u^+)$	1618 (10.4)	1667 (10.6)	1572 (Jacox ,1994)
$\omega_3 (\Pi_u)$	456 (22.8)	445 (25.7)	440 (Jacox ,1994)

Tetraatomic ion MgH₃⁻

The properties of the tetraatomic ion are displayed in Table 17. Its geometrical structure is shown in Fig. 10 *b*. The tetraatomic ion MgH_3^- has the planar equilibrium configuration of the D_{3h} symmetry. The computed values determined through two methods are generally in agreement with each other. The reference experimental data for comparison are not available.

Table 17. Properties of tetraatomic MgH$_3^-$ ion, D_{3h} symmetry

Property	DFT/B3PW91	MP2
R_e(M−H)	1.816	1.807
α_e(H−M−H)	120	120
−E	201.83437	201.51157
ω_1 (A')	1328 (0)	1393 (0)
ω_2 (A_2'')	552 (21.6)	581 (24.1)
ω_3 (E')	597 (24.5)	613 (26.9)
ω_4 (E')	1249 (44.2)	1312 (44.0)

(a)   (b)

Figure 10. Equilibrium geometrical structure of the species: (a) MgH$_2$ $D_{\infty h}$; (b) MgH$_3^-$, D_{3h}

3.3.2 *Geometrical Structure and Vibrational Spectra of Pentaatomic Molecules LiMgH$_3$ and NaMgH$_3$*

For pentaatomic MMgH$_3$ molecules two probable isomeric geometrical structures, cyclic (C_{2v}) and linear ($C_{\infty v}$), were considered. For each configuration the geometric parameters were optimized and the frequencies of normal vibrations were computed. The obtained parameters of the cyclic (C_{2v}) and linear ($C_{\infty v}$) configuration are displayed in Tables 18 and 19 respectively. Their equilibrium geometrical structures are shown in Figure 11.

It is worth to compare the internuclear separations (terminal and bridged) between these complex hydrides with the lower molecules, MgH$_2$ and MgH$_3^-$. For MgH$_3^-$ the bond lengths and angles are equivalent, R_e(Mg−H) ≈ 1.81 Å (Table 16) while in the MMgH$_3$ molecules the bridge distances R_e(Mg−H) are increased to 1.85 − 1.88 Å; and the terminal distance is reduced to ~1.72 Å; the bond angles become also non−equivalent, the angle β_e(H$_4$−Mg$_1$−H$_5$) decreases to 87° in LiMgH$_3$ and 95° in NaMgH$_3$. So far, the internuclear distance, R_e (Mg−H) of MgH$_2$ is the smallest among the species.

Comparing the MMgH$_3$ molecules with those of our previous study given in Chapter two MBeH$_3$, it can be noticed that molecules of both types have the most intensive band

corresponding to the stretching vibrations in LiBeH$_3$ (1528 cm^{-1} by DFT) and LiMgH$_3$ (1127 cm^{-1} by MP2). Also, for magnitudes of their frequencies the MBeH$_3$ configuration possessed much higher frequencies.

The IR spectra of MMgH$_3$ molecules displayed in Figure 12 (a) and (b) have been analyzed. There are some relationship of the vibration frequency modes observed for LiMgH$_3$ and NaMgH$_3$. For example, the bending vibrations are observed at the frequency, ω_9 for LiMgH$_3$ (391 cm^{-1}) and NaMgH$_3$ (368 cm^{-1}) corresponding to the MgH$_3$ moiety. Another similarity is seen at the ω_5 having vibration frequencies of 663 cm^{-1} LiMgH$_3$ and 617 cm^{-1} NaMgH$_3$ corresponding to the wagging vibrations. However, for both hydrides the highest frequency is observed to correspond to stretching vibrations at 1622 cm^{-1} (LiMgH$_3$) and 1589 cm^{-1} (NaMgH$_3$). Another important thing to note in these IR spectra characteristics is availability of more peaks to the NaMgH$_3$ hydride than LiMgH$_3$ hydride.

Table 18. Properties of MMgH$_3$ (M= Li, Na) molecules (C_{2v})

	LiMgH$_3$		NaMgH$_3$	
Property	**DFT/B3PW91**	**MP2**	**DFT/B3PW91**	**MP2**
R_{e1} (Mg$-$H$_1$)	1.876	1.865	1.865	1.854
R_{e2} (Mg$-$H$_2$)	1.718	1.713	1.727	1.722
R_{e3} (M$-$H$_1$)	1.743	1.743	2.115	2.144
β_e (H$_1$$-Mg-H_1$)	87.2	87.1	95.1	94.7
α_e (H$_1$$-M-H_1$)	95.5	95.0	81.1	80.3
$-E$	209.35322	209.00109	364.08288	363.50689
ω_1 (A$_1$)	1582 (5.88)	1622 (6.03)	1559 (6.50)	1589 (6.67)
ω_2 (A$_1$)	1280 (4.72)	1319 (5.30)	1253 (10.2)	1297 (11.1)
ω_3 (A$_1$)	1102 (17.63)	1127 (20.4)	965 (12.8)	1013 (14.65)
ω_4 (A$_1$)	450 (0.14)	458 (0.16)	267 (0.28)	273 (0.28)
ω_5 (B$_1$)	643 (15.1)	664 (16.9)	594 (16.8)	617 (19.1)
ω_6 (B$_1$)	282 (1.67)	285 (1.69)	244 (0.77)	238 (0.84)
ω_7 (B$_2$)	1092 (19.29)	1127 (17.3)	1112 (14.7)	1149 (14.9)
ω_8 (B$_2$)	1014 (1.67)	1045 (3.02)	801 (8.03)	845 (9.13)
ω_9 (B$_2$)	376 (4.71)	391 (5.17)	351 (3.31)	368 (3.82)

Table 19. Properties of MMgH$_3$ (M= Li, Na) molecules ($C_{\infty v}$)

Property	LiMgH$_3$		NaMgH$_3$	
	DFT/B3PW91	MP2	DFT/B3PW91	MP2
R_{e1} (Mg−H$_1$)	1.690	1.685	1.694	1.688
R_{e2} (Mg−H$_2$)	1.715	1.708	1.722	1.712
R_{e3} (M−H$_2$)	1.841	1.809	2.243	2.209
R_{e4} (M−H$_3$)	1.623	1.617	1.921	1.926
$-E$	209.30471	208.95242	364.03534	363.45646
$\Delta_r E_{iso}$	127.4	127.8	124.7	132.4
ω_1 (Σ^+)	1740 (15.2)	1804 (14.6)	1664 (15.4)	1721 (16.1)
ω_2 (Σ^+)	1661 (2.53)	1710 (3.01)	1644 (0.003)	1699 (0.77)
ω_3 (Σ^+)	1338 (8.41)	1376 (8.84)	1122 (9.61)	1153 (10.7)
ω_4 (Σ^+)	257 (0.02)	275 (0.03)	149 (0.09)	157 (0.002)
ω_5 (Π)	561 (12.4)	566 (26.64)	658 (20.12)	761 (21.0)
ω_6 (Π)	248 (0.19)	239 (0.02)	231 (0.18)	245 (1.10)
ω_7 (Π)	68 (10.0)	66 (21.96)	90 (21.8)	87 (24.7)

Note: $\Delta_r E_{iso}$ is the relative energy of linear isomer regarding cyclic, $\Delta_r E_{iso} = E_{lin} - E_{cycl}$, in kJ mol^{-1}

The existence of linear isomer MMgH$_3$ was reported in (Li *et al.*, 2009) for lithium bonding complexes HMgH⋯LiH. In this study, MMgH$_3$ linear isomers similar to those of MBeH$_3$ have much higher energy than the cyclic one, *i. e.* by 128 and 132 kJ mol^{-1} (MP2) for LiMgH$_3$ and NaMgH$_3$ respectively. But still there are no imaginary frequencies here thus linear structure corresponds to the minimum potential energy surface, this is quite different from MBeH$_3$ as it was reported in Chapter two. Henceforth, for further investigation of thermodynamic properties of MMgH$_3$ hydrides only the cyclic isomer was considered.

(a)   (b)
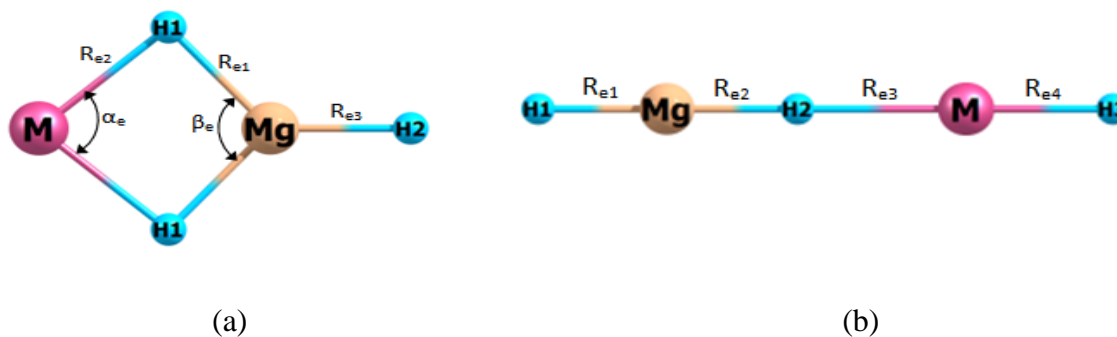
Figure 11. Equilibrium geometrical structure of MMgH$_3$ (M = Li, Na) molecules: (a) cyclic, C_{2v}; (b) linear, $C_{\infty v}$

(a)   (b)
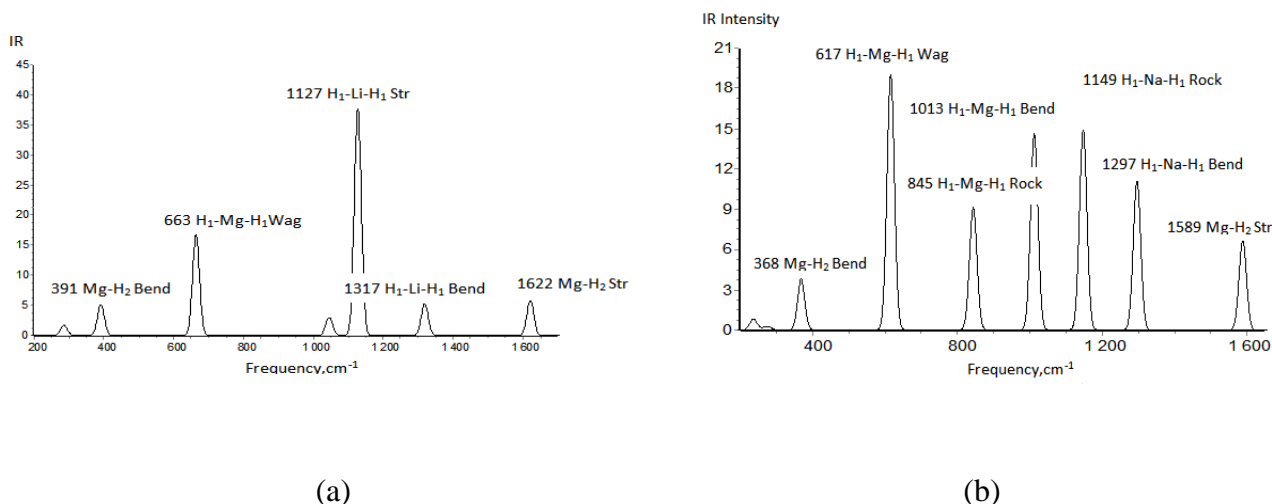
Figure 12. IR spectra of MMgH$_3$ (M= Li, Na) molecules, C_{2v} isomer, calculated by MP2: (a) LiMgH$_3$, (b) NaMgH$_3$

3.3.3 Geometrical Structure and Vibrational Spectra of Heptaatomic Li$_2$MgH$_4$ and Na$_2$MgH$_4$ Molecules

Different geometrical shapes of the M$_2$MgH$_4$ molecules have been considered; a polyhedral (compact or "hat"−shaped), C_{2v}; two−cycled, D_{2d}; and hexagonal, C_{2v} and bipyramidal one with a tail of C_{2v} symmetry. Among these four configurations the last one was found to be unstable as imaginary vibrational frequencies were observed. The rest three structures were proved to correspond to the minima at the potential energy surface and therefore appeared to be isomers of M$_2$MgH$_4$ molecules. Hereafter these isomers are denoted as I, II, and III, for C_{2v} compact, D_{2d}, and C_{2v} hexagonal, respectively; the equilibrium geometrical configurations are shown in Fig. 13 and the parameters are displayed in Tables 20−22.

(a)   (b)   (c)
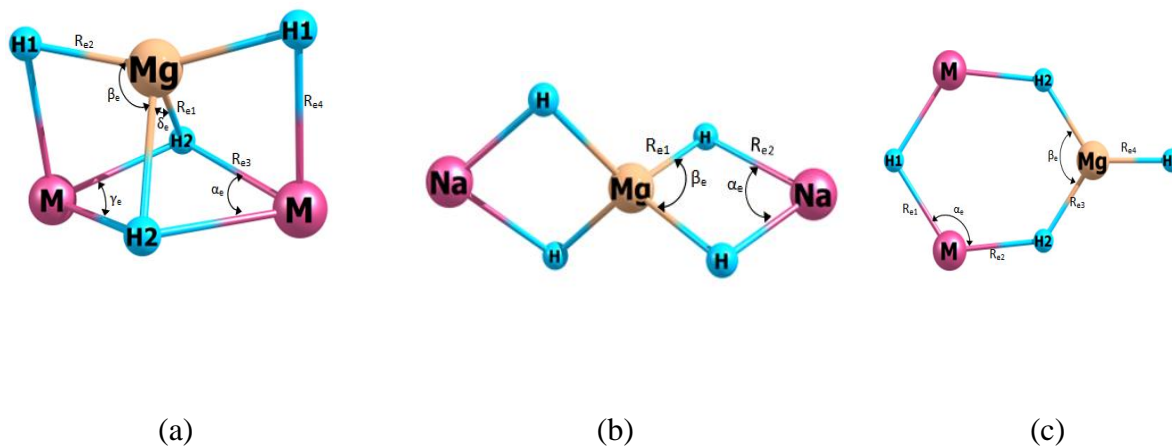
Figure 13. Equilibrium geometrical configurations of M$_2$MgH$_4$ isomers: (a) polyhedral (C_{2v}); (b) two−cycled (D_{2d}); (c) hexagonal (C_{2v})

30

Table 20. Properties of M_2MgH_4 (M= Li, Na) molecules (C_{2v}, compact hat−shaped structure)

Property	Li$_2$MgH$_4$		Na$_2$MgH$_4$	
	DFT/B3PW91	MP2	DFT/B3PW91	MP2
R_{e1}(Mg−H$_2$)	2.020	2.010	2.008	1.995
R_{e2}(Mg−H$_1$)	1.782	1.778	1.800	1.795
R_{e3}(M−H$_2$)	1.858	1.857	2.270	2.260
R_{e4}(M−H$_1$)	1.957	1.948	2.280	2.276
α_e(H$_2$−M−H$_1$)	91.1	91	79.3	79.1
γ_e(H$_2$−M−H$_2$)	79.4	79.1	69.8	69.3
β_e(H$_1$−Mg−H$_2$)	91.3	91.4	99.2	99.2
δ_e(H$_2$−Mg−H$_2$)	71.9	72.1	80.4	80.3
$-E$	217.49095	217.08743	526.94830	526.09871
μ_e	2.9	2.9	6.5	6.8
ω_1 (A_1)	1400 (0.03)	1442 (0.01)	1346 (0.61)	1388 (0.54)
ω_2 (A_1)	1134 (2.39)	1184 (2.36)	1039 (5.65)	1090 (5.51)
ω_3 (A_1)	850 (17.6)	884 (19.7)	982 (17.1)	814 (24.8)
ω_4 (A_1)	724 (14.6)	745 (16.3)	708 (8.64)	737 (9.68)
ω_5 (A_1)	497 (0.13)	507 (0.13)	290 (0.21)	297 (0.21)
ω_6 (A_1)	272 (0.02)	276 (0.03)	123 (0.04)	129 (0.05)
ω_7 (A_2)	901 (0)	924 (0)	763 (0)	798 (0)
ω_8 (A_2)	450(0)	465(0)	316(0)	339(0)
ω_9 (B_1)	929 (16.7)	958 (17.5)	865 (13.8)	903 (14.7)
ω_{10} (B_1)	297 (3.09)	301 (3.14)	678 (16.9)	709 (19.7)
ω_{11} (B_2)	1409 (14.2)	1444 (15.2)	1341 (17.5)	1379 (18.7)
ω_{12} (B_2)	982 (17.1)	1009 (19.3)	873 (16.8)	913 (20.0)
ω_9 (B_2)	766 (6.41)	797 (8.72)	468 (0.36)	498 (0.31)
ω_{14} (B_2)	545 (0.63)	55 (0.70)	291 (0.92)	298 (0.98)
ω_{15} (B_2)	479 (0.36)	492 (0.49)	220 (1.05)	244 (1.26)

Table 21. Properties of M_2MgH_4 (M = Li, Na) molecules (D_{2d})

Property	Li$_2$MgH$_4$		Na$_2$MgH$_4$	
	DFT/B3PW91	MP2	DFT/B3PW91	MP2
R_{e1}(Mg−H)	1.888	1.881	1.8902	1.883
R_{e2}(M−H)	1.741	1.734	2.098	2.096
α_e(H−M−H)	97.1	96.8	83.8	83
β_e(H−Mg−H)	87.4	87.2	95.5	95.1
$-E$	217.49511	217.09378	526.95022	526.10086
$\Delta_r E_{iso}$(I−II)	−10.9	−16.7	−5.0	−5.6
ω_1 (A_1)	372.(0)	386 (0)	430 (0)	442(0)
ω_2 (B_1)	1258.(0)	1301 (0)	1222 (0)	1263 (0)
ω_3 (B_1)	1100.(0)	1139 (0)	989 (0)	1018 (0)
ω_4 (B_1)	391.(0)	397 (0)	192 (0)	195 (0)
ω_5 (B_2)	1232 (3.77)	1270 (4.2)	1157 (14.7)	1189 (15.9)
ω_6 (B_2)	1061 (45.6)	1098 (44.4)	968 (37.0)	998 (40.0)
ω_7 (B_2)	496 (0.25)	507 (0.28)	327 (0.59)	332 (0.63)
ω_8 (E)	1071 (41.2)	1098 (48.8)	1039 (32.2)	1072 (31.7)
ω_9 (E)	1007 (0.22)	1047 (0.02)	845 (19.1)	871 (24.9)
ω_{10} (E)	614 (18.1)	635 (20.2)	527 (13.2)	544 (14.9)
ω_{11} (E)	111 (1.01)	116 (1.06)	61 (1.94)	59 (2.12)

Note: $\Delta_r E_{iso}$(I−II) is the energy of isomerization reaction M_2MgH_4 (I, $C_{2v, comp}$)= M_2MgH_4 (II, D_{2d}), $\Delta_r E_{iso}$(I−II) = E(II) – E(I), in kJ·mol^{-1}

The IR spectra of three isomers of Li$_2$MgH$_4$ and Na$_2$MgH$_4$ molecules are presented in Fig. 14. By comparing IR spectra of Li$_2$MgH$_4$ and Na$_2$MgH$_4$ molecules, alike features may be observed for the isomers of the same symmetry. For the polyhedral isomer I, the bands of high intensity at 885 cm^{-1}, 746 cm^{-1} (Li$_2$MgH$_4$) correspond to H−Li−H wagging and bending vibrations and 903 cm^{-1} (Na$_2$MgH$_4$) correspond to H−Mg−H asymmetrical stretching vibrations of MgH$_2$ moiety. However, similar H−Mg−H asymmetrical stretching vibrations are observed at 1444 cm^{-1} (Li$_2$MgH$_4$) and 1379 cm^{-1} (Na$_2$MgH$_4$) for polyhedral isomer I. For the two−cycled D_{2d} isomer, similar wagging vibration is observed at 635 cm^{-1} to the H−Li−H (Li$_2$MgH$_4$) and Na−H−Mg (Na$_2$MgH$_4$). The most intensive band in spectrum of Li$_2$MgH$_4$ D_{2d} is seen at 1098 cm^{-1} and corresponds to the H−Li−H rocking mode, in Na$_2$MgH$_4$ D_{2d} is observed at 998 cm^{-1} corresponding to the H−Mg−H bending vibration. In this two−cycled D_{2d} isomer, Li$_2$MgH$_4$ has few peaks of vibration modes compared to Na$_2$MgH$_4$. For the hexagonal isomer the most intense

bands appear at 627 cm^{-1} (Li$_2$MgH$_4$) and 590 cm^{-1} (Na$_2$MgH$_4$) and are characterized by wagging modes of the MgH$_4$ fragment. Other similarities may be noted between two hexagonal species as rocking vibrations at 848 cm^{-1} (MgH$_3$), bending vibration at 971 cm^{-1} H−Mg−H (Li$_2$MgH$_4$) and 716 cm^{-1}, 796 cm^{-1} for same fragment H−Mg−H (Na$_2$MgH$_4$) respectively.

Table 22. Properties of M$_2$BeH$_4$ (M = Li, Na) molecules (C_{2v}, hexagonal structure)

Property	Li$_2$MgH4		Na$_2$MgH4	
	DFT/B3PW91	MP2	DFT/B3PW91	MP2
R_{e1}(M−H$_1$)	1.706	1.701	2.045	2.049
R_{e2}(M−H$_2$)	1.717	1.709	2.058	2.063
R_{e3}(Mg−H$_2$)	1.837	1.829	1.833	1.824
R_{e4}(Mg−H$_3$)	1.725	1.72	1.734	1.730
α_e(H$_1$−M−H$_2$)	130.8	129.9	122.7	121.5
β_e(H$_2$−Mg−H$_2$)	106.2	105.5	107.5	107.2
$-E$	217.495891	217.09565	526.95285	526.10334
$\Delta_r E_{iso}$(I–III)	−2.0	−21.6	−6.9	−12.1
μ_e	4.9	5.1	5.9	6.2
ω_1 (A_1)	1566 (3.66)	1597 (2.73)	1536 (4.84)	1564 (3.83)
ω_2 (A_1)	1436 (23.4)	1493 (25.7)	1398 (20.0)	1451 (21.6)
ω_3 (A_1)	990 (3.90)	1019 (3.41)	847 (0.004)	872 (0.003)
ω_4 (A_1)	949 (9.71)	971 (10.9)	777 (19.2)	795 (20.8)
ω_5 (A_1)	370 (0.78)	380 (0.76)	215 (0.06)	222 (0.08)
ω_6 (A_1)	270 (0.61)	282 (0.68)	156 (0.30)	160 (0.32)
ω_7 (A_2)	284 (0)	307 (0)	226 (0)	235 (0)
ω_8 (B_1)	599 (21.8)	627 (23.9)	560 (20.6)	590 (23.2)
ω_9 (B_1)	382 (0.19)	396 (0.29)	312 (3.03)	324 (3.68)
ω_{10} (B_1)	165 (1.99)	169 (2.23)	141 (2.07)	144 (2.13)
ω_{11} (B_2)	1381 (9.00)	1435 (9.09)	1337 (12.5)	1389 (13.6)
ω_{12} (B_2)	1242 (9.53)	1279 (10.7)	992 (8.95)	1033 (9.95)
ω_{13} (B_2)	831 (12.3)	847 (13.4)	702 (14.7)	716 (16.0)
ω_{14} (B_2)	400 (4.86)	413 (5.37)	361 (1.80)	371 (1.90)
ω_{15} (B_2)	186 (0.98)	211 (0.95)	80 (0.82)	96 (0.87)

Note: $\Delta_r E_{iso}$(I–III) is the energy of isomerization reaction M$_2$MgH$_4$ (I, $C_{2v,\ comp}$) = M$_2$MgH$_4$ (III, $C_{2v,\ hex}$), $\Delta_r E_{iso}$(I–III) = E(III) – E(I), in kJ mol^{-1}

The relative energies $\Delta_r E_{iso}$ of the isomers II and III regarding I given in Tables 21, 22 were calculated for the following isomerization reactions:

$$M_2MgH_4 \, (I, \, C_{2v, \, comp}) = M_2MgH_4 \, (II, \, D_{2d}) \qquad (12)$$

$$M_2MgH_4 \, (I, \, C_{2v, \, comp}) = M_2MgH_4 \, (III, \, C_{2v, \, hex}). \qquad (13)$$

The values of $\Delta_r E_{iso}$ are negative: for reaction (12) -16.7 kJ mol^{-1} (Li$_2$MgH$_4$), -5.6 kJ mol^{-1} (Na$_2$MgH$_4$), and for (13) -21.6 kJ mol^{-1} (Li$_2$MgH$_4$), -12.1 kJ mol^{-1} (Na$_2$MgH$_4$) according to MP2 calculations. Therefore among three isomers, I, II, and III, the first one has the highest energy, followed by D_{2d}, and the hexagonal: $E(I) > E(II) > E(III)$ for both molecules.

The relative concentrations p_A/p_B has been calculated the same way as it was explained in Chapter two for the temperature range between 500 and 2000 K. The plots are shown in Fig. 15.

a   b
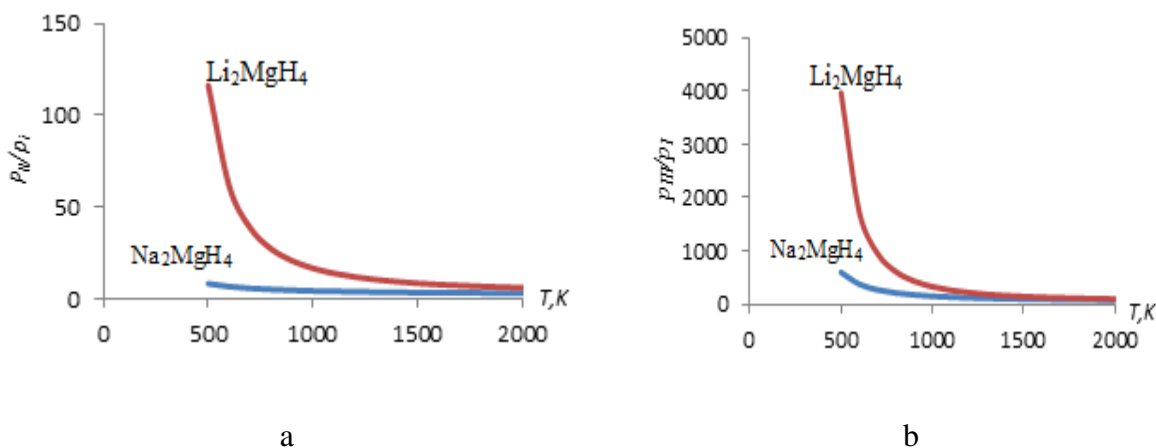
Figure 14. Relative abundance p_A/p_B versus temperature for three isomers of complex hydrides M_2MgH_4 by MP2 method: (a) $p_{II}(D_{2d})/p_I(C_{2v}, comp)$ (b) $p_{III}(C_{2v}, hex)/p_I(C_{2v}, comp)$
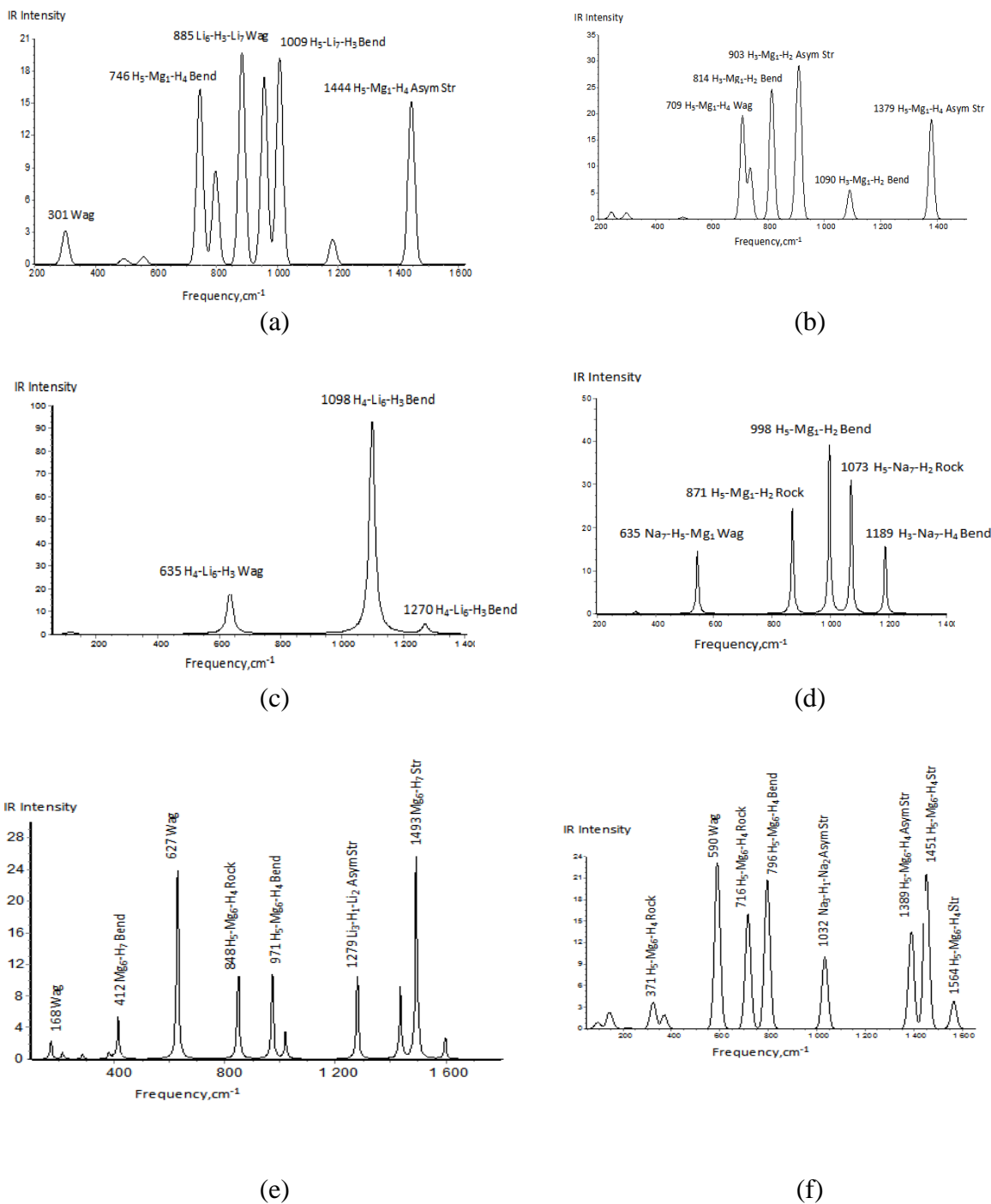
Figure 15. IR spectra of complex hydrides M_2MgH_4 (M = Li, Na) calculated by MP2: (a) Li_2MgH_4 (C_{2v}, compact); (b) Na_2MgH_4 (C_{2v}, compact); (c) Li_2MgH_4 (D_{2d}); (d) Na_2MgH_4 (D_{2d}); (e) Li_2MgH_4 (C_{2v}, hexagonal); (f) Na_2MgH_4 (C_{2v}, hexagonal)

It is seen that the relative concentrations of the isomers II and III decrease with temperature rise for both molecules; above the 1500 K the decay is slow. Table 23 shows the values of p_A/p_B for selected two temperatures, 500 K and 1000 K. The values of p_{II}/p_I and p_{III}/p_I are much bigger than

35

1, hence the relative amount of the isomer I is much smaller compared to both II and III.

Table 23. The values of p_A/p_B for selected two temperatures, 500 K and 1000 K

Isomerization reaction	$\Delta_r E_{iso}$ kJ mol^{-1}	$\Delta_r \varepsilon$ kJ mol^{-1}	$\Delta_r H(0)$, kJ mol^{-1}	p_A/p_B $T=500$ K	p_A/p_B $T=1000$ K
Li$_2$MgH$_4$(I, $C_{2v, comp}$) = Li$_2$MgH$_4$(II, D_{2d})	−16.7	− 0.6	−17.3	116.4	16.8
Li$_2$MgH$_4$(I, $C_{2v, comp}$) = Li$_2$MgH$_4$(III, $C_{2v, hex}$)	−21.6	−3.4	−25.0	3969	326.2
Na$_2$MgH$_4$(I, $C_{2v, comp}$) = Na$_2$MgH$_4$(II, D_{2d})	−5.6	−0.04	−5.6	8.5	4.6
Na$_2$MgH$_4$(I, $C_{2v, comp}$) = Na$_2$MgH$_4$(III, $C_{2v, hex}$)	−12.1	−3.4	−15.6	594.9	147.8

The fraction of each isomer of M$_2$MgH$_4$ was estimated as $x_i = p_i/(p_I + p_{II} + p_{III})$ where i stands for I, II, or III, the results for selected temperatures are given in Table 24. Thus as depicted the hexagonal isomer of Na$_2$MgH$_4$ is predominant in a broad temperature range and its concentration decreases gradually with temperature raise while for the rest of the isomers their concentration is very small and they seem to increase very slowly with temperature raise. Figure 6 shows the fraction of isomers I, II, III in equilibrium vapour.

Table 24. The fraction of x$_i$ of isomers I, II, III in equilibrium vapour: (a) Li$_2$MgH$_4$; (b) Na$_2$MgH$_4$

Species	T, K	x_1	x_2	x_3
Li$_2$MgH$_4$	500	0.0002	0.028	0.971
	1000	0.003	0.049	0.948
Na$_2$MgH$_4$	500	0.002	0.014	0.984
	1000	0.007	0.030	0.964

a   b
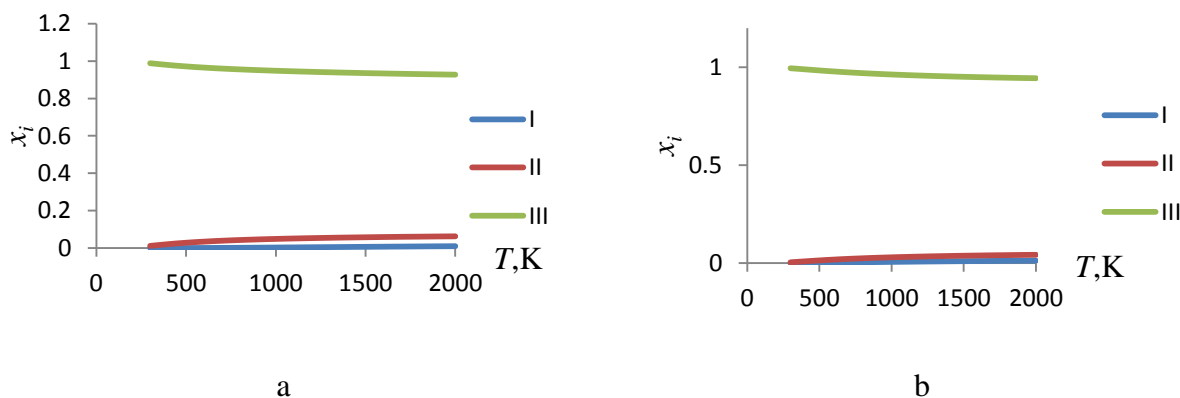
Figure 16. The fraction of x$_i$ of isomers I, II, III in equilibrium vapour: (a) Li$_2$MgH$_4$; (b) Na$_2$MgH$_4$

3.4 Thermodynamic Properties of Complex Hydrides

3.4.1. The Enthalpies of Dissociation Reactions and Enthalpies of Formation of Molecules

Several enthalpies of dissociation reactions and enthalpies of formation of the complex hydrides $MMgH_3$ and M_2MgH_4 have been examined. The hexagonal isomer of C_{2v} symmetry of M_2MgH_4 was revealed to have the lowest energy. The results of calculation of the energies and enthalpies of gas−phase reactions for DFT/B3PW91 and MP2 methods are tabulated in Tables 25 and 26. A partial dissociation and complete reduction reactions of the complex hydrides, $MMgH_3$ and M_2MgH_4 which led to the release of hydrogen gas were investigated. The calculated values of $\Delta_r H°(0)$ depict all reactions were accompanied with the absorption of energy (endothermic). The partial dissociation of both penta− and heptaatomic hydrides required much less energy than reaction with hydrogen formation. It was observed that some of the reactions worked well at the expense of much energy than others. H_2 evolving (reactions 2 for $MMgH_3$ and 5, for M_2MgH_4) and dissociation into ionic subunits M_2H^+ and MgH_3^- (reactions 8) were seen to consume much energy. The similar result was reported earlier for $MBeH_3$ and M_2BeH_5 in Chapter two.

The enthalpies of formation $\Delta_f H°(0)$ of the complex hydrides were computed through the enthalpies of the reactions and enthalpies of formation of the gaseous products Li, Na, H_2, LiH and NaH (Gurvich *et al*., 1992−2000) as it was done in chapter two. The enthalpies of formation of $MMgH_3$ molecules are accepted as the averaged values found through the enthalpies of reactions 1 and 2; likewise for M_2MgH_4 through reactions 3−5. Uncertainties were estimated as half−differences between maximum and minimum magnitudes. The accepted values of $\Delta_f H°(0)$ are gathered in Table 27.

In order to determine the stability of the gaseous complex hydrides $MMgH_3$ and M_2MgH_4 the heterophase decomposition which led to hydrogen release were also examined. The enthalpies of the heterophase reactions were computed and shown in Table 28. The enthalpies of formation of all species involved in the reaction in condensed phase were obtained from (Gurvich *et al*., 1992−2000). For all six heterophase reactions enumerated in the calculations, magnesium and alkali metals are in solid state for all reactions, while some alkali metal hydrides are in gas−phase (reactions 1, 4) or in condensed phase (reactions 2, 5). Reactions 3 and 6 are for complete decomposition. The results show that only one reaction in which gaseous MH is among the products is endothermic (reaction 4), while the remaining reactions are exothermic; the largest energy being released in reactions 2 and 5 with $MH_{(c)}$.

Table 25. The energies and enthalpies of gas−phase dissociation reactions, and enthalpies of formation of gaseous complex hydrides LiMgH$_3$ and Li$_2$MgH$_4$; all values are given in kJ mol^{-1}

	Reaction	Method	$\Delta_r E$	$\Delta_r \varepsilon$	$\Delta_r H°(0)$	$\Delta_f H°(0)$
1	LiMgH$_3$ = LiH + Mg + H$_2$	DFT/B3PW91	159.92	−12.01	147.92	137.43
		MP2	156.63	−12.36	144.27	141.07
2	LiMgH$_3$ = Li + Mg + 3/2H$_2$	DFT/B3PW91	163.49	−7.16	156.33	147.31
		MP2	148.40	−7.40	140.10	162.64
3	Li$_2$MgH$_4$ = LiMgH$_3$ + LiH	DFT/B3PW91	178.51	−10.95	167.55	115.72
		MP2	190.14	−11.66	178.48	104.78
4	Li$_2$MgH$_4$ = 2LiH + Mg + H$_2$	DFT/B3PW91	338.43	−22.96	315.47	100.90
		MP2	346.77	−24.02	322.76	105.30
5	Li$_2$MgH$_4$ = 2Li + Mg + 2H$_2$	DFT/B3PW91	345.57	−13.27	332.29	129.08
		MP2	330.31	−14.10	349.32	145.16
6	Li$_2$MgH$_4$ = 2LiH + MgH$_2$	DFT/B3PW91	356.86	−24.70	332.15	
		MP2	376.75	−25.99	350.75	
7	Li$_2$MgH$_4$ = Li$_2$H$_2$ + MgH$_2$	DFT/B3PW91	155.77	−10.42	145.36	
		MP2	168.83	−11.29	157.54	
8	Li$_2$MgH$_4$ = Li$_2$H$^+$ + MgH$_3^-$	DFT/B3PW91	564.74	−15.53	549.21	
		MP2	575.89	−15.72	560.17	

Table 26. The energies and enthalpies of gas−phase dissociation reactions, and enthalpies of formation of gaseous complex hydrides NaMgH$_3$ and Na$_2$MgH$_4$; all values are given in kJ mol^{-1}

	Reaction	Method	$\Delta_r E$	$\Delta_r \varepsilon$	$\Delta_r H°(0)$	$\Delta_f H°(0)$
1	NaMgH$_3$ = NaH + Mg + H$_2$	DFT/B3PW91	139.60	−9.30	130.30	158.41
		MP2	142.50	−10.02	132.47	156.23
2	NaMgH$_3$ = Na + Mg + 3/2H$_2$	DFT/B3PW91	91.14	−3.13	88.01	165.65
		MP2	77.91	−3.60	74.31	179.36
3	Na$_2$MgH$_4$ = NaMgH$_3$ + NaH	DFT/B3PW91	152.30	−7.88	144.42	160.81
		MP2	165.53	−8.17	157.35	147.87
4	Na$_2$MgH$_4$ = 2NaH + Mg + H$_2$	DFT/B3PW91	291.91	−17.18	274.20	199.05
		MP2	307.87	−18.20	289.67	200.07
5	Na$_2$MgH$_4$ = 2Na + Mg + 2H$_2$	DFT/B3PW91	195.00	−4.84	190.16	171.27
		MP2	178.54	−5.35	173.19	188.24
6	Na$_2$MgH$_4$ = 2NaH + MgH$_2$	DFT/B3PW91	310.34	−18.93	291.42	
		MP2	337.84	−20.17	317.67	
7	Na$_2$MgH$_4$ = Na$_2$H$_2$ + MgH$_2$	DFT/B3PW91	161.34	−9.89	174.61	
		MP2	174.61	−9.97	164.63	
8	Na$_2$MgH$_4$ = Na$_2$H$^+$ + MgH$_3^-$	DFT/B3PW91	473.47	−10.80	462.67	
		MP2	480.21	−10.54	469.68	

Table 27. Accepted enthalpies of formation (in kJ mol^{-1}) of gaseous complex hydrides MMgH$_3$ and M$_2$MgH$_4$ (M = Li, Na)

Hydride	$\Delta_f H°(0)$	Hydride	$\Delta_f H°(0)$
LiMgH$_3$	144 ± 13	NaMgH$_3$	162 ± 11
Li$_2$MgH$_4$	113 ± 12	Na$_2$MgH$_4$	175 ± 26

Table 28. The enthalpies of heterophase dissociation reactions of gaseous hydrides MMgH$_3$ and M$_2$MgH$_4$

No	Reaction	$\Delta_r H°(0)$, kJ mol^{-1}	
		M = Li	M = Na
1	MMgH$_3$ = MH$_{(g)}$ + Mg$_{(c)}$ + H$_{2(g)}$	−4	−20
2	MMgH$_3$ = MH$_{(c)}$ + Mg$_{(c)}$ + H$_{2(g)}$	−229	−214
3	MMgH$_3$ = M$_{(c)}$ + Mg$_{(c)}$ + 3/2H$_{2(g)}$	−144	−162
4	M$_2$MgH$_4$ = 2MH$_{(g)}$ + Mg$_{(c)}$ + H$_{2(g)}$	166	111
5	M$_2$MgH$_4$ = 2MH$_{(c)}$ + Mg$_{(c)}$ + H$_{2(g)}$	−285	−279
6	M$_2$MgH$_4$ = 2M$_{(c)}$ + Mg$_{(c)}$ + 2H$_{2(g)}$	−113	−175

3.4.2 Thermal Stability of the Complex Hydrides and Thermodynamic Favourability of the Reactions

The thermodynamic stability of the complex hydrides MMgH$_3$ and M$_2$MgH$_4$ was investigated through Gibbs free energies for heterophase reactions shown in Table 28. The temperature dependences of $\Delta_r G°(T)$ are presented in Figs. 17−19. For the reactions in which MH is in gaseous phase, $\Delta_r G°(T)$ values are negative at moderate and elevated temperatures (Fig. 17); the decomposition reactions are thermodynamically favoured at temperatures above 200 K (NaMgH$_3$), 300 K (LiMgH$_3$), 700 K (Na$_2$MgH$_4$) and 900 K (Li$_2$MgH$_4$). Thus the MMgH$_3$ hydrides appeared to be less stable thermodynamically than M$_2$MgH$_4$ and Na−containing hydrides are less stable compared to Li−hydrides.

For reactions in which both MH and Mg are in condensed phase (Fig. 18) the values of $\Delta_r G°(T)$ are negative for whole temperature range considered. The Na−containing hydrides are slightly more stable than Li−hydrides as the values of $\Delta_r G°(T)$ for the former are less negative. The inflections on the curves correspond to phase change transition of the products, namely the melting points of LiH$_{(c)}$ and NaH$_{(c)}$ at 965 K and 911 K (Gurvich *et al.*, 1992−2000) respectively. The Gibbs free energy for the decomposition reaction of MMgH$_3$ decreases with temperature raise, while for M$_2$MgH$_4$ hydrides the values of $\Delta_r G°$ pass through maximum at temperatures of

the phase transitions. Here the entropy has an impact on $\Delta_r G°(T)$: as a jump of entropy at phase transition of $MH_{(c)}$ occurs hence the contribution of entropy factor $T\Delta_r S$ increases with temperature raise.

(a)   (b)
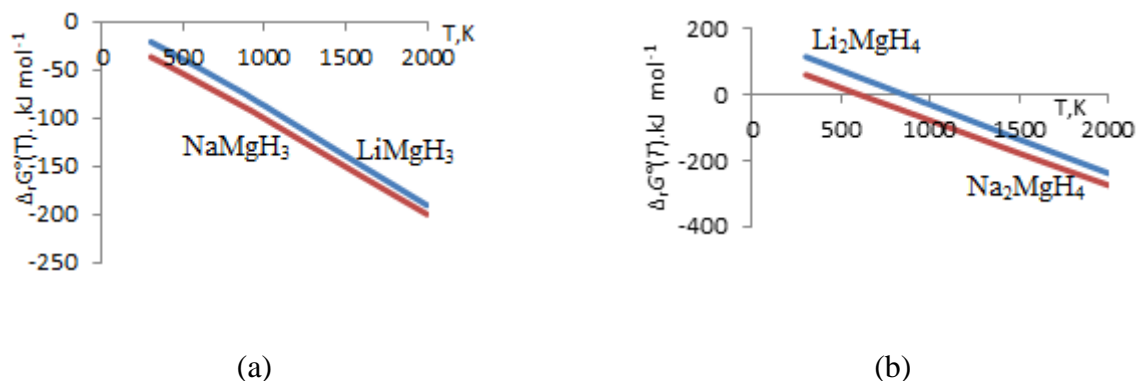
Figure 17. Gibbs free energy $\Delta_r G°(T)$ against temperature for heterophase decomposition reactions of complex hydrides MMgH$_3$ and M$_2$MgH$_4$: (a) MMgH$_3$(g) = MH(g) + Mg(c) + H$_2$(g); (b) M$_2$MgH$_4$(g) = 2MH(g) + Mg(c) + H$_2$(g)

(a)   (b)
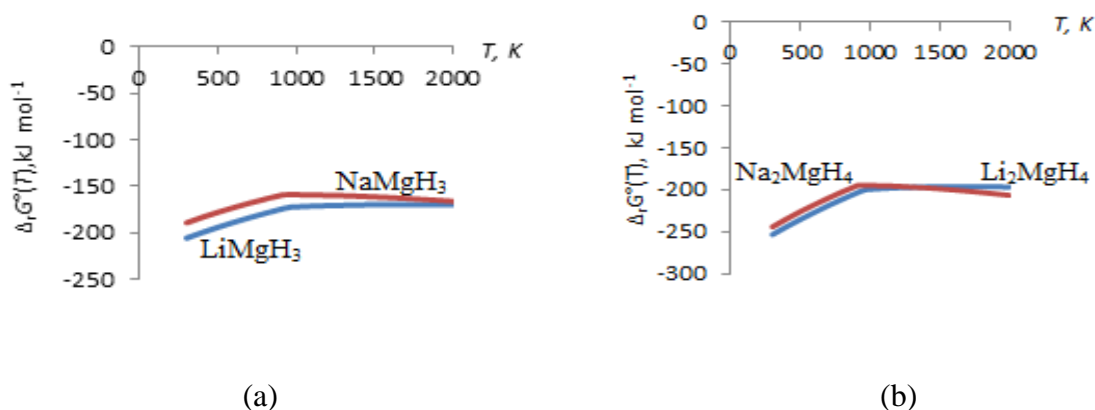
Figure 18. Gibbs free energy $\Delta_r G°(T)$ against temperature for heterophase decomposition reactions of complex hydrides MMgH$_3$ and M$_2$MgH$_4$: (a) MMgH$_3$(g) = MH$_{(c)}$ + Mg(c) + H$_2$(g); (b) M$_2$MgH$_4$(g) = 2MH(c) + Mg(c) + H$_2$(g)

Considering the reactions which dissociate to condensed phase metal hydride and magnesium for the whole temperature range selected the values of Gibbs free energies (Fig. 19) are negative and decrease with the temperature increase implying that the decomposition processes are spontaneous. It is quite different from the first case (Fig. 18), the Na−containing hydrides are less stable than Li−hydrides as the values of $\Delta_r G°(T)$ are less negative for the latter.

For different channels of dissociation of the hydrides, a correlation between $\Delta_r G°(T)$ and $\Delta_r H°(0)$ values may be noted: the lower is the enthalpy of the reaction the more negative are $\Delta_r G°(T)$ and hence the more favourable the decomposition process. For instance, for the reactions with gaseous alkali hydrides MH the enthalpies $\Delta_r H°(0)$ are positive, ~111−166 kJ mol^{-1} (M$_2$MgH$_4$);

40

then the Gibbs free energies are positive at low and moderate temperatures and turn negative at certain temperatures said (Fig. 17). This implies that the reversibility of the reactions is able to be achieved. For other heterogeneous reactions the $\Delta_r H°(0)$ values are negative, the Gibbs free energies are negative (Figs. 18, 19) that is the decomposition of the hydrides, both $MMgH_3$ and M_2MgH_4, is spontaneous in the whole temperature range considered. The reaction with Li/Na and Mg in condensed phase the reversibility may be achieved by pressure increase (Le Châtelier's principle). The reversibility of the decomposition reactions of hydrides is one of the requirements for hydrogen storage materials.

(a)   (b)
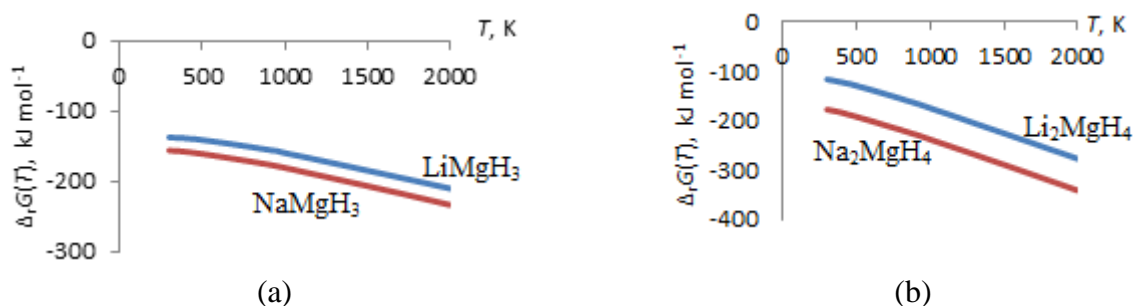
Figure 19. Gibbs free energy $\Delta_r G°(T)$ against temperature for heterophase decomposition reactions of complex hydrides $MMgH_3$ and M_2MgH_4: (a) $MMgH_3(g) = M(c) + Mg(c) + 3/2H_2(g)$; (b) $M_2MgH_4(g) = 2M(c) + Mg(c) + 2H_2(g)$

3.5 Conclusion

The optimized geometrical parameters, vibrational spectra and thermodynamic properties of the complex hydrides $MMgH_3$ and M_2MgH_4 (M = Li, Na) and subunits have been determined using DFT/B3PW91 and MP2 methods. The calculated results obtained by both methods are in a good agreement with the reference data available for subunits. Different channels of dissociation reactions were considered; for partial dissociation and complete reduction of hydrogen gas. The enthalpies of formation of the complex hydrides were found. For testing thermal stabilities of the studied complex hydrides, the Gibbs free energies $\Delta_r G°(T)$ of heterophase decomposition of $MMgH_3$ and M_2MgH_4 with hydrogen release were analyzed. It was revealed that the results obtained for these species were in accordance with our previous results discussed in chapter two. In summary, the reactions of complete decomposition were observed to be spontaneous at a broad temperature range and the reversibility of the reactions might be achieved if some criteria are observed. The complex hydrides $MMgH_3$ and M_2MgH_4 (M = Na or Li) similar to $MBeH_3$ and M_2BeH_4 may also be considered as promising candidates for hydrogen storage purposes as they showed the feasibility of hydrogen gas production.

CHAPTER FOUR

4.1 GENERAL DISCUSSION ON THE PROPERTIES OF COMPLEX HYDRIDES MXH$_3$ and M$_2$XH$_4$ (M = Li, Na; X = Be, Mg)

4.1.1 Geometrical properties of complex hydrides and their subunits

The optimized geometrical parameters and geometrical structures of the hydrides MBeH$_3$, MMgH$_3$, M$_2$BeH$_4$, M$_2$MgH$_4$ (M= Li, Na) and respective subunits MH, M$_2$H$^+$, M$_2$H$_2$, BeH$_2$, MgH$_2$, MgH$_3^-$, BeH$_3^-$ have been computed and analyzed using DFT/B3PW91 and MP2 methods with the basis set 6−311++G(d,p). A comparison with the available experimental data has been done in order to test the accuracy of the calculated results particularly for lower species. The obtained results showed that the two methods are in good agreement with each other and available experimental data.

Two possible geometrical configurations of MBeH$_3$ and MMgH$_3$ complex hydrides were investigated and confirmed to exist, the cyclic of C_{2v} and linear structure of $C_{\infty v}$ symmetry. The cyclic structure was proved to be equilibrium one. For linear configuration of LiBeH$_3$, the imaginary frequency was revealed while for both molecules the linear configuration was proved to possess much higher energy (~130 kJ mol^{-1}) compared to C_{2v}. Unlike pentaatomic molecules, for M$_2$BeH$_4$ and M$_2$MgH$_4$ complex hydrides three isomers were proved to exist; polyhedral (compact or "hat"−shaped), C_{2v}; two−cycled, D_{2d}; and hexagonal, C_{2v}. For M$_2$BeH$_4$ and M$_2$MgH$_4$ the lowest energy was found for the compact and cyclic hexagonal configuration respectively. The relative abundance of the isomers in saturated vapour was analysed. The results showed striking features to the compact isomer of Li$_2$BeH$_4$ molecule; it was more abundant at moderate temperatures, but at higher temperatures its concentration was seen to decrease. The hexagonal isomer was more abundant compared to either isomers (compact and D_{2d}) for Na$_2$BeH$_4$.

4.1.2 Vibrational spectra

The fundamental vibration frequencies and IR intensities for all molecules involved in this study were computed and the vibration spectra of some selected molecules were visualized and analyzed. Different molecular vibrational modes of the complex hydrides were examined by use of the Chemcraft and wxMcMolPlt software. The following assigned molecular vibration modes

were observed in our study, symmetrical and asymmetrical stretching, wagging, bending and rocking as displayed in Figs.; 3, 5, 12 and 14. Some similarities of the bands were observed for isomers of the same configurations. For instance, in Fig. 3 the stretching vibrations were observed at the frequencies 2029 cm^{-1} and 1980 cm^{-1} for LiBeH$_3$ and NaBeH$_3$ and assigned to the stretching Be−H vibrational modes. The similarities in spectra are due to alike fragments (XH$_2$ or XH$_4$) and similar geometry of the species.

4.1.3 Thermodynamic properties

Various channels of dissociation reactions of the complex hydrides had been examined in order to determine the most probable channels. As it has been already pointed out earlier, that the hexagonal isomer of C_{2v} symmetry for M$_2$MgH$_4$ and the compact isomer of C_{2v} symmetry for M$_2$BeH$_4$ were found to possess the lowest energy and therefore the energies of these two isomers were used in calculation of energies of the dissociation reactions respectively. Two different types of dissociation reactions were examined, the partial and complete reduction of hydrogen gas. The calculated values of $\Delta_r H°(0)$ showed that all the reactions were associated with the absorption of energy (endothermic). The enthalpies of formation of the complex hydrides were estimated through the enthalpies of the gaseous reactions; the enthalpies of the reactants were taken from the database and trustful literature resources. The enthalpies of formation of the complex hydrides were displayed in Table 29.

Table 29. The enthalpies of formation of gaseous complex hydrides

Hydride	$\Delta_f H°(0)$	Hydride	$\Delta_f H°(0)$
LiBeH$_3$	105 ± 26	LiMgH$_3$	144 ± 13
Li$_2$BeH$_4$	63 ± 37	Li$_2$MgH$_4$	113 ± 12
NaBeH$_3$	121 ± 27	NaMgH$_3$	162 ± 11
Na$_2$BeH$_4$	117 ± 39	Na$_2$MgH$_4$	175 ± 26

Some of regularities may be observed in Fig. 20 in which the enthalpies of formations of MXH$_3$ and M$_2$XH$_4$ are depicted. The similarity is seen between magnesium and beryllium; also beryllium based hydrides have lower enthalpies compared to magnesium based hydride.
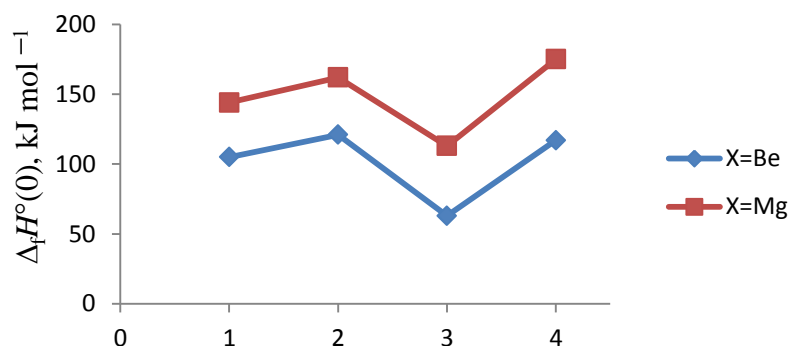
Figure 20. The enthalpies of formation MXH$_3$ and M$_2$XH$_4$; 1–LiXH$_3$; 2–NaXH$_3$; 3–Li$_2$XH$_4$; 4–Na$_2$XH$_4$

The thermodynamic stability of the complex hydrides MBeH$_3$, MMgH$_3$, M$_2$BeH$_4$, M$_2$MgH$_4$ was examined through Gibbs free energies for different heterophase reactions. Two aggregate states of metal hydride and central metal atom were considered; for the reactions in which MH was in gas phase the values of Gibbs free energy were found to be negative at moderate and elevated temperatures while for the reactions in which both MH and central metal atom were in condensed phase the values of Gibbs free energy were negative for the whole temperature range selected. The inflections on curves were observed to correspond to the phase transition of the products, the melting points of NaH(c) and LiH(c) at 911 K and 965 K, respectively.

4.2 CONCLUSION

Theoretical study by DFT/B3PW91 and MP2 methods has been performed for the complex hydrides, MBeH$_3$, MMgH$_3$, M$_2$BeH$_4$ and M$_2$MgH$_4$ (M= Li, Na) in vapour form. The geometrical parameters and vibration frequencies of the molecules were exploited for computing thermodynamic functions and properties. Three isomers of the complex hydrides M$_2$BeH$_4$ and M$_2$MgH$_4$ and two of MBeH$_3$ and MMgH$_3$ were found. The enthalpies of the dissociation reactions of the complex hydrides were determined and these enthalpies were employed in the determination of enthalpies of formation. The stability of the complex hydrides was assessed using Gibbs free energies of heterophase decomposition reactions. The results revealed that the reactions of complete reduction of hydrogen were spontaneous at a broad temperature range. It was suggested that the reversibility of the reactions could be attained under certain conditions. The studied complex hydrides may be considered as appropriate materials for hydrogen storage application.

4.3 RECOMENDATIONS

The theoretical study of the complex hydrides, $LiBeH_3$, $NaBeH_3$ $LiMgH_3$, $NaMgH_3$, Na_2BeH_4, Li_2BeH_4, Li_2MgH_4 and Na_2MgH_4 have been performed. Bell and Coates were the first to synthesize experimentally the Li_2BeH_4 compound.

It is recommended that the synthesis of other complex hydrides should be performed. Keeping in mind that the properties discussed in these complex hydrides can be a good way forward towards the experimental synthesis of the hydrides. The experimental studies of thermochemical properties of gaseous and solid complex hydrides need to be performed.

REFERENCES

Ahluwalia, R., Hua, T., and Peng, J. (2012). On−board and off−board performance of hydrogen storage options for light−duty vehicles. *International Journal of Hydrogen Energy*. 37(3): p. 2891−2910.

Alapati, S. V., Johnson, J. K., and Sholl, D. S. (2006). Identification of destabilized metal hydrides for hydrogen storage using first principles calculations. *Journal of Physical Chemistry. B*. 110(17): p. 8769−8776.

Amsler, M., Flores−Livas, J. A., Huan, T. D., Botti, S., Marques, M. A., and Goedecker, S. (2012). Novel structural motifs in low energy phases of LiAlH$_4$. *Physical review letters*. 108(20): p. 205505.

Armaroli, N., Balzani, V. (2011). *Chemical and Sustainable Chemistry*. 4: p. 21.

Becke, A. D. (1993). Density‐functional thermochemistry. III. The role of exact exchange. *Journal of Physical Chemistry. B*. 98(7): p. 5648−5652.

Bell, N. and Coates, G. (1968). Lithium and sodium beryllium hydrides. *Journal of the Chemical Society A: Inorganic, Physical, Theoretical*, 628−631.

Bode, B. M. and Gordon M. S. (1998). MacMolPlt: a graphical user interface for GAMESS. *Journal of Molecular Graphics Modelling.*, 16(3): p. 133−138.

Bogdanović, B. and Schwickardi, M. (1997). Ti−doped alkali metal aluminium hydrides as potential novel reversible hydrogen storage materials. *Journal .of Alloys and Compound*. 7. 253: p. 1−9.

Chater, P. A. (2010). Mixed anion complex hydrides for hydrogen storage. University of Birmingham.

Chen, Y. L., Huang C. H., and Hu, W. P. (2005). Theoretical study on the small clusters of LiH, NaH, BeH$_2$, and MgH$_2$. *Journal of Physical Chemistry A*. 109(42): p. 9627−9636.

Dinca, I. M. and Long, J. R. (2008). Hydrogen storage in microporous metal–organic frameworks with exposed metal sites. *Angewandte Chemie International Edition*, 47, 6766−6779.

Fletcher, G., Schmidt, M., and Gordon, M. (1999). Developments in parallel electronic structure

theory. *Advanced Chemical Physical*. 110: p. 267−294.

Giri, S., Behera, S. and Jena, P. (2014). Superalkalis and superhalogens as building blocks of supersalts. *The Journal of Physical Chemistry A*. 118, 638−645.

Graetz, J. (2012). Metastable Metal Hydrides for Hydrogen Storage. *ISRN Materials Science*.

Granovsky, A. A., Firefly version 8.1.0, www

Grochala, W. and Edwards, P. P. (2004). Thermal decomposition of the non−interstitial hydrides for the storage and production of hydrogen. *Chemical Reviews*, 104, 1283−1316.

Gross, K. J. (2000) In−situ X−ray diffraction study of the decomposition of NaAlH$_4$. *Journal of Alloys and Compounds*. 297(1): p. 270−281.

Gurvich, L.V., Yungman, V. S., Bergman, G. A., Veitz, I. V., Gusarov, A. V., Iorish V. S., Leonidov, V. Y., Medvedev, V. A., Belov, G. V., Aristova, N. M., Gorokhov, L. N., Dorofeeva, O. V., Ezhov, Y. S., Efimov, M. E., Krivosheya, N. S., Nazarenko, I. I, Osina, E. L., Ryabova, V. G., Tolmach, P. I., Chandamirova, N. E., and Shenyavskaya, E. A. (1992−2000)."Thermodynamic Properties of individual Substances. Ivtanthermo for Windows Database on Thermodynamic Properties of Individual Substances and Thermodynamic Modeling Software", Version 3.0 (Glushko Thermocenter of RAS, Moscow.

http://classic.chem.msu.su/gran/firefly/index.html

Hu, C., Wang, Y., Chen, D., Xu, D. and Yang, K. (2007). First−principles calculations of structural, electronic, and thermodynamic properties of Na$_2$BeH$_4$. *Physical Review B*, 76, 144104.

Huber, K. P.; Herzberg, G. (1979). Molecular Spectra and Molecular Structure. IV. Constants of Diatomic Molecules Van Nostrand Reinhold Co.

Ikeda, K., Kogure, Y., Nakamori, Y., and Orimo, S. (2005). Reversible hydriding and dehydriding reactions of perovskite−type hydride NaMgH$_3$. *Scripta materialia*. 53(3): p. 319−322.

Irikura, K. K. (2007) "Experimental Vibrational Zero−Point Energies: Diatomic Molecules" *Journal of Physical Chemistry*. Ref. Data 36(2), 389.

Jacox, M. E. (1994). Vibrational and Electronic Energy Levels of Polyatomic Transient

Molecules. *Journal of Physical Chemistry*. Ref. Data, Monograph 3 (updated data in NIST Chemistry Webbook − http://webbook.nist.gov/chemistry/.

Jena, P. (2015). Superhalogens: A Bridge between Complex Metal Hydrides and Li Ion Batteries. *The Journal of Physical Chemistry Letters*, 6, 1119−1125.

Li, Q., Wang, Y., Li, W., Cheng, J., Gong, B., and Sun, J. (2009). Prediction and characterization of the HMgHLiX (X= H, OH, F, CCH, CN, and NC) complexes: a lithium–hydride lithium bond. *Physical Chemistry Chemical Physics*. 11(14): p. 2402−2407.

Meisner, G., Tibbetts, G., Pinkerton, F., Olk, C., and Balogh, M. (2002). Enhancing low pressure hydrogen storage in sodium alanates. *Journal of Alloys and Compound*. 337(1): p. 254−263.

Milliken, J. (2007). Hydrogen, Fuel Cells and Infrastructure Technologies Program: Multiyear Research, Development and Demonstration Plan. National Renewable Energy Laboratory (NREL), Golden, CO.

Morioka, H., Kakizaki, H., Chung, S. C., and Yamada, A. (2003). Reversible hydrogen decomposition of $KAlH_4$. *Journal of Alloys and Compound*. 353(1): p. 310−314.

Nakamori, Y., Miwa, K., Ninomiya, A., Li, H., Ohba, N., Towata S. I., Züttel, A. and Orimo, S. I. (2006) Correlation between thermodynamical stabilities of metal borohydrides and cation electronegativites: First−principles calculations and experiments. Phys. Rev. B. 74(4): p. 045126.

NIST Chemistry Webbook (http://webbook.nist.gov/chemistry).

NIST Diatomic Spectral Database (www.physics.nist.gov/PhysRefData/MolSpec/Diatomic/index.html).

Palumbo, M., Torres, F., Ares, J., Pisani, C., Fernandez, J., and Baricco, M. (2007) Thermodynamic and ab initio investigation of the Al–H–Mg system. *Calphad*. 31(4): p. 457−467.

Pathak, B., Samanta, D., Ahuja, R. and Jena, P. (2011). Borane Derivatives: A New Class of Super-and Hyperhalogens. *Chemical and Physical Chemistry*, 12, 2423−2428.

Patlitzianas, K. D., Doukas, H., Kagiannas, A. G., and Psarras, J. (2008). Sustainable energy

policy indicators: Review and recommendations. *Renewable Energy*. 33(5): p. 966−973.

Reardon, H., Mazur, N., and Gregory, D. H. (2013). Facile synthesis of nanosized sodium magnesium hydride, NaMgH$_3$. *Progres in Natural Science: Materials International*. 23(3): p. 343−350.

Riis, T., Sandrock, G., Ullebeg, O., and Vie, P. J. (2005). Hydrogen Storage–Gaps and Priorities. HIA HCG Storage paper. 11.

Sandrock, G., Gross, K., and Thomas, G. Effect of Ti−catalyst content on the reversible hydrogen storage properties of the sodium alanates. *Journal of Alloys and Compound*, 2002. 339(1): p. 299−308.

Sartbaeva, A., Kuznetsov, V., Wells, S., and Edwards, P. (2011). *Energy Environment Sciences* 2008, 1, 79

Schmidt, M. W., Baldridge, K. K., Boatz, J. A., Elbert, S. T., Gordon, M. S., Jensen, J. H., Koseki, S., Matsunaga, K. A., Nguyen, K. A. and Su, S. General atomic and molecular electronic structure system. *Journal of Computational Chemistry*. 1993. 14(11): p. 1347−1363.

Shomari, A., Pogrebnaya, T. P., Pogrebnoi, A. M. (2016). Gaseous Metal Hydrides MBeH$_3$ and M$_2$BeH$_4$ (M = Li, Na): Quantum Chemical Study of Structure, Vibrational Spectra and Thermodynamic Properties. *International Journal of Materials Science and Applications*. Vol. 5. pp. 5−17. doi: 10.11648/j.ijmsa.20160501.12.

Sun, D., Kiyobayashi, H. T., Takeshita, H. T., Kuriyama, N., and Jensen, C. M. (2002). X−ray diffraction studies of titanium and zirconium doped NaAlH$_4$: elucidation of doping induced structural changes and their relationship to enhanced hydrogen storage properties. *Journal of Alloys and Compounds*. 337(1): p. L8−L11.

Tokarev, K. L. (2007-2009) "OpenThermo", v. 1.0 Beta 1 (C) ed. http://openthermo.software.informer.com/.

Tsere M. H., Pogrebnaya, T. P., Pogrebnoi, A. M. (2015). Complex Hydrides Li2MH5 (M = B, Al) for Hydrogen Storage Application: Theoretical Study of Structure, Vibrational Spectra and Thermodynamic Properties. *International Journal of Computational and Theoretical Chemistry*. Vol. 3, No. 6, 2015, pp. 58−67. doi: 10.11648/j.ijctc.20150306.13.

Union, E. (2008). Energy and Environment Agency. Copenhagen: Office for Official Publications of the European Communities.

Vajeeston, P., Ravindran, P., and Fjellvag, H. (2008). Electronic structural and lattice dynamical properties of hydrides. in Proceedings of the *International Conference on Materials Science Research and Nanotechnology*. Kodaikanal, India.

Vajeeston, P., Ravindran, P., Kjekshus, A., and Fjellvåg, H. (2008). First−principles investigations of the $MMgH_3$ (M= Li, Na, K, Rb, Cs) series. *Journal of Alloys and Compound*. 450(1): p. 327−337.

Wu, C. and Ihle, H. (1982). Thermochemistry of the Dimer Lithium Hydride Molecule Li_2H_2 (g).

Zaluska, A., Zaluski, L., and Ström−Olsen, J. (1999). Nanocrystalline magnesium for hydrogen storage. *Journal of Alloys and Compound*. 288(1): p. 217−225.

Zaluski, L., Zaluska, A. and Ström−Olsen, J. (1999). Hydrogenation properties of complex alkali metal hydrides fabricated by mechano−chemical synthesis. *Journal of Alloys and Compound*. 290(1): p. 71−78.

Zhou, L. (2005). Progress and problems in hydrogen storage methods. *Renewable and Sustainable Energy Reviews*, 9, 395−408.

Zhurko, G. and Zhurko, D. (2013). Chemcraft, Version 1.7 (build 365).

Zidan, R. A., Takara S., Hee, A. G., and Jensen, C. M. (1999). Hydrogen cycling behavior of zirconium and titanium−zirconium−doped sodium aluminum hydride. *Journal of Alloys and Compound*. 285(1): p. 119−122.

Züttel, A. (2003). Materials for hydrogen storage. *Materials today*, 6, 24−33.

Züttel, A., Wenger, P., Rentsch, S., Sudan, P., Mauron, P., and Emmenegger, C. (2003) $LiBH_4$ a new hydrogen storage material. *Journal of Power Sources*. 118(1): p. 1−7.

LIST OF APPENDICES

The thermodynamic functions of the complex hydrides Li_2BeH_4, Li_2MgH_4, Na_2BeH_4 and Na_2MgH_4 in gaseous phase were calculated using Openthermo software. The required geometrical parameter and vibrational frequencies were calculated by MP2 method. The thermodynamic functions computed are: the molar heat capacity $c_p°(T)$; Gibbs reduced free energy $\Phi°(T)$; entropy $S°(T)$; and enthalpy increment $H°(T)–H°(0)$. The units are J mol^{-1}K^{-1} for c_p, $\Phi°$, $S°$, and kJ mol^{-1} for $H°(T)–H°(0)$.

Table A 1. Thermodynamic functions of Li$_2$BeH$_4$, (C_{2v}, compact)

T, K	$c°_p(T)$	$S°(T)$	$H°(T)– H°(0)$	$\Phi°(T)$
200	52.627	229.890	7.850	190.641
300	70.957	254.681	14.026	207.928
400	88.009	277.490	21.996	222.501
500	102.070	298.699	31.526	235.647
600	113.070	318.324	42.307	247.812
700	121.540	336.419	54.057	259.195
800	128.050	353.093	66.550	269.905
900	133.080	368.478	79.617	280.014
1000	137.030	382.712	93.131	289.581
1100	140.150	395.923	106.995	298.655
1200	142.650	408.228	121.138	307.280
1300	144.680	419.728	135.507	315.492
1400	146.340	430.512	150.060	323.326
1500	147.710	440.657	164.764	330.814
1600	148.870	450.227	179.594	337.981
1700	149.840	459.282	194.531	344.852
1800	150.650	467.871	209.557	351.450
1900	151.350	476.036	224.659	357.794
2000	152.000	483.816	239.828	363.902

Table A 2. Thermodynamic functions of Na$_2$BeH$_4$, ($C_{2v,}$ compact)

T, K	$c^\circ_p(T)$	$S^\circ(T)$	$H^\circ(T)- H^\circ(0)$	$\Phi^\circ(T)$
200	63.097	264.296	9.100	218.796
300	80.148	293.134	16.270	238.901
400	95.598	318.363	25.077	255.671
500	108.330	341.116	35.297	270.522
600	118.260	361.784	46.648	284.037
700	125.870	380.611	58.872	296.509
800	131.680	397.815	71.762	308.113
900	136.150	413.595	85.163	318.969
1000	139.660	428.129	98.961	329.168
1100	142.410	441.573	113.069	338.783
1200	144.610	454.062	127.423	347.876
1300	146.390	465.709	141.976	356.497
1400	147.850	476.613	156.690	364.692
1500	149.050	486.855	171.536	372.498
1600	150.060	496.508	186.493	379.950
1700	150.920	505.631	201.542	387.077
1800	151.600	514.277	216.670	393.905
1900	152.230	522.493	231.865	400.459
2000	152.770	530.316	247.117	406.758

Table A 3.Thermodynamic functions of Li$_2$MgH$_4$, ($C_{2v,}$ compact)

T, K	$c^\circ_p(T)$	$S^\circ(T)$	$H^\circ(T)- H^\circ(0)$	$\Phi^\circ(T)$
200	61.223	244.520	8.434	202.351
300	83.492	273.661	15.696	221.341
400	101.460	300.258	24.985	237.796
500	114.790	324.410	35.833	252.744
600	124.440	346.240	47.821	266.539
700	131.440	365.977	60.633	279.358
800	136.590	383.882	74.048	291.322
900	140.450	400.203	87.909	302.526
1000	143.390	415.160	102.107	313.053
1100	145.680	428.938	116.565	322.970
1200	147.470	441.692	131.225	332.338
1300	148.920	453.555	146.046	341.212
1400	150.070	464.635	160.997	349.637
1500	151.050	475.023	176.055	357.653
1600	151.850	484.797	191.200	365.297
1700	152.500	494.022	206.418	372.600
1800	153.060	502.756	221.698	379.590
1900	153.530	511.046	237.030	386.293
2000	153.980	518.933	252.407	392.730

Table A 4. Thermodynamic functions of Li$_2$MgH$_4$, (C_{2v}, compact)

T, K	$c^\circ_p(T)$	$S^\circ(T)$	$H^\circ(T)- H^\circ(0)$	$\Phi^\circ(T)$
200	72.841	278.616	9.974	228.748
300	93.226	312.124	18.307	251.101
400	109.310	341.258	28.473	270.077
500	121.060	366.985	40.024	286.938
600	129.450	389.841	52.573	302.220
700	135.500	410.275	65.836	316.223
800	139.910	428.671	79.618	329.149
900	143.190	445.349	93.781	341.148
1000	145.690	460.571	108.230	352.341
1100	147.630	474.551	122.900	362.824
1200	149.160	487.464	137.742	372.679
1300	150.370	499.452	152.720	381.975
1400	151.340	510.633	167.807	390.771
1500	152.160	521.103	182.984	399.114
1600	152.850	530.945	198.234	407.049
1700	153.400	540.228	213.546	414.613
1800	153.860	549.010	228.910	421.838
1900	154.260	557.340	244.318	428.752
2000	154.630	565.263	259.763	435.382

Table A 5. Thermodynamic functions of Li$_2$BeH$_4$, (D_{2d})

T, K	$c^\circ_p(T)$	$S^\circ(T)$	$H^\circ(T)- H^\circ(0)$	$\Phi^\circ(T)$
200	57.864	238.907	9.198	192.917
300	72.853	265.125	15.715	212.742
400	88.319	288.228	23.782	228.772
500	101.880	309.439	33.313	242.813
600	112.820	329.020	44.070	255.571
700	121.340	347.079	55.796	267.371
800	127.920	363.730	68.273	278.389
900	133.020	379.103	81.330	288.736
1000	137.000	393.332	94.839	298.493
1100	140.150	406.543	108.702	307.723
1200	142.660	418.849	122.847	316.477
1300	144.700	430.351	137.219	324.798
1400	146.370	441.138	151.775	332.727
1500	147.760	451.285	166.483	340.296
1600	148.920	460.858	181.317	347.535
1700	149.880	469.916	196.258	354.470
1800	150.720	478.507	211.288	361.125
1900	151.410	486.674	226.395	367.519
2000	152.030	494.457	241.568	373.673

Table A 6. Thermodynamic functions of Na$_2$BeH$_4$, (D_{2d})

T, K	$c°_p(T)$	$S°(T)$	$H°(T) - H°(0)$	$Φ°(T)$
200	65.487	293.424	10.788	239.484
300	80.478	322.763	18.075	262.514
400	95.294	347.980	26.876	280.790
500	107.93	370.650	37.059	296.532
600	117.940	391.252	48.374	310.629
700	125.650	410.038	60.570	323.509
800	131.540	427.217	73.442	335.414
900	136.070	442.984	86.833	346.503
1000	139.600	457.511	100.624	356.887
1100	142.380	470.951	114.728	366.653
1200	144.600	483.439	129.081	375.872
1300	146.390	495.086	143.634	384.598
1400	147.850	505.990	158.348	392.884
1500	149.050	516.233	173.196	400.769
1600	150.080	525.887	188.154	408.291
1700	150.920	535.011	203.205	415.479
1800	151.640	543.659	218.335	422.362
1900	152.270	551.875	233.531	428.964
2000	152.790	559.699	248.785	435.307

Table A 7. Thermodynamic functions of Li$_2$MgH$_4$, (D_{2d})

T, K	$c°_p(T)$	$S°(T)$	$H°(T) - H°(0)$	$Φ°(T)$
200	65.959	251.580	9.731	202.924
300	84.041	281.745	17.232	224.305
400	100.550	308.252	26.486	242.038
500	113.660	332.164	37.226	257.712
600	123.440	353.797	49.106	271.954
700	130.620	373.393	61.828	285.068
800	135.940	391.200	75.169	297.239
900	139.920	407.451	88.970	308.595
1000	142.950	422.357	103.120	319.237
1100	145.310	436.096	117.538	329.243
1200	147.160	448.822	132.165	338.685
1300	148.640	460.663	146.958	347.618
1400	149.840	471.724	161.886	356.091
1500	150.850	482.098	176.922	364.150
1600	151.670	491.861	192.049	371.830
1700	152.330	501.077	207.252	379.164
1800	152.950	509.802	222.518	386.181
1900	153.450	518.085	237.837	392.908
2000	153.860	525.967	253.203	399.366

Table A 8.Thermodynamic functions of Na$_2$MgH$_4$, (D_{2d})

T, K	$c°_p(T)$	$S°(T)$	$H°(T)- H°(0)$	$\Phi°(T)$
200	73.587	287.582	11.045	232.356
300	91.726	320.870	19.317	256.482
400	107.580	349.514	29.311	276.235
500	119.670	374.888	40.705	293.478
600	128.420	397.523	53.134	308.967
700	134.730	417.820	66.308	323.094
800	139.340	436.128	80.024	336.098
900	142.760	452.747	94.137	348.150
1000	145.350	467.928	108.548	359.380
1100	147.360	481.879	123.188	369.890
1200	148.920	494.771	138.005	379.767
1300	150.190	506.743	152.962	389.080
1400	151.190	517.911	168.033	397.887
1500	152.040	528.371	183.195	406.241
1600	152.710	538.205	198.433	414.184
1700	153.310	547.482	213.734	421.756
1800	153.760	556.258	229.089	428.986
1900	154.190	564.584	244.488	435.906
2000	154.530	572.503	259.927	442.540

Table A 9. Thermodynamic functions of Li$_2$BeH$_4$, (C_{2v}, hexagonal)

T, K	$c°_p(T)$	$S°(T)$	$H°(T)- H°(0)$	$\Phi°(T)$
200	70.278	251.753	9.884	202.331
300	86.163	283.371	17.736	224.251
400	99.129	309.995	27.022	242.441
500	109.740	333.296	37.484	258.329
600	118.290	354.089	48.901	272.587
700	125.120	372.857	61.085	285.593
800	130.550	389.932	73.878	297.584
900	134.850	405.566	87.157	308.725
1000	138.320	419.961	100.822	319.139
1100	141.100	433.279	114.797	328.918
1200	143.370	445.657	129.024	338.137
1300	145.240	457.208	143.457	346.856
1400	146.770	468.029	158.060	355.129
1500	148.070	478.200	172.803	362.998
1600	149.150	487.791	187.665	370.500
1700	150.060	496.862	202.626	377.670
1800	150.850	505.462	217.673	384.533
1900	151.520	513.6370	232.793	391.114
2000	152.120	521.425	247.977	397.437

Table A 10. Thermodynamic functions of Na$_2$BeH$_4$, (C_{2v} hexagonal)

T, K	$c^\circ_p(T)$	$S^\circ(T)$	$H^\circ(T)- H^\circ(0)$	$\Phi^\circ(T)$
200	80.362	295.011	11.744	236.290
300	94.541	330.361	20.510	261.993
400	106.260	359.221	30.571	282.795
500	115.690	383.984	41.685	300.613
600	123.210	405.768	53.645	316.360
700	129.190	425.228	66.276	330.548
800	133.940	442.801	79.442	343.499
900	137.710	458.802	93.031	355.434
1000	140.740	473.474	106.959	366.515
1100	143.180	487.006	121.159	376.861
1200	145.170	499.552	135.579	386.570
1300	146.800	511.238	150.179	395.716
1400	148.150	522.167	164.928	404.361
1500	149.280	532.427	179.800	412.560
1600	150.220	542.092	194.777	420.356
1700	151.020	551.225	209.841	427.789
1800	151.680	559.877	224.979	434.889
1900	152.290	568.097	240.182	441.685
2000	152.840	575.923	255.440	448.203

Table A 11. Thermodynamic functions of Li$_2$MgH$_4$, (C_{2v} hexagonal)

T, K	$c^\circ_p(T)$	$S^\circ(T)$	$H^\circ(T)- H^\circ(0)$	$\Phi^\circ(T)$
200	75.693	263.666	10.1777	212.778
300	92.973	297.795	18.6532	235.618
400	106.480	326.464	28.6511	254.836
500	117.170	351.422	39.856	271.711
600	125.410	373.547	52.003	286.875
700	131.700	393.373	64.873	300.697
800	136.490	411.286	78.293	313.420
900	140.170	427.584	92.134	325.213
1000	143.040	442.507	106.300	336.207
1100	145.290	456.250	120.721	346.504
1200	147.090	468.972	135.343	356.186
1300	148.550	480.805	150.128	365.322
1400	149.740	491.858	165.044	373.969
1500	150.730	502.224	180.068	382.179
1600	151.550	511.978	195.182	389.989
1700	152.230	521.186	210.372	397.438
1800	152.810	529.905	225.625	404.558
1900	153.310	538.181	240.933	411.374
2000	153.760	546.057	256.288	417.913

Table A 12. Thermodynamic functions of Na$_2$MgH$_4$, (C_{2v}, hexagonal)

T, K	$c^\circ_p(T)$	$S^\circ(T)$	$H^\circ(T) - H^\circ(0)$	$\Phi^\circ(T)$
200	85.159	301.651	11.911	242.098
300	101.130	339.337	21.259	268.473
400	113.580	370.210	32.021	290.159
500	123.150	396.631	43.879	308.873
600	130.380	419.755	56.573	325.467
700	135.810	440.280	69.895	340.430
800	139.910	458.695	83.690	354.082
900	143.040	475.363	97.845	366.647
1000	145.460	490.565	112.275	378.290
1100	147.370	504.522	126.921	389.139
1200	148.890	517.412	141.736	399.299
1300	150.110	529.379	156.688	408.850
1400	151.100	540.541	171.750	417.862
1500	151.930	550.995	186.902	426.394
1600	152.630	560.823	202.131	434.491
1700	153.210	570.093	217.422	442.198
1800	153.660	578.863	232.766	449.549
1900	154.090	587.184	248.156	456.576
2000	154.470	595.098	263.585	463.306